Petrogenesis of the Volcanic and Intrusive Rocks Associated with the Bingham Canyon Porphyry Cu-Au-Mo Deposit, Utah

KIMBERLY A. WAITE, JEFFREY D. KEITH, ERIC H. CHRISTIANSEN

Brigham Young University, Provo, Utah

JAMES A. WHITNEY

University of Georgia, Athens, Georgia

KEIKO HATTORI

University of Ottawa, Ottawa, Ontario, Canada

DAVID G. TINGEY

Brigham Young University, Provo, Utah

CHRISTOPHER J. HOOK

University of Georgia, Athens, Georgia

Abstract

Recent examination of volcanic rocks near the Bingham Canyon Cu-Au-Mo deposit, Utah, suggests that primitive alkaline magmas are an important factor in the formation of this world-class porphyry copper deposit. The Bingham deposit is spatially associated with a monzonitic intrusive complex emplaced at 39 to 37 Ma into Paleozoic sedimentary rocks. Coeval igneous rocks vented to the surface and formed a volcanic pile, part of which is preserved on the eastern flank of the Oquirrh Mountains.

Bingham volcanic rocks are divided into three chrono-lithologic suites: an older volcanic suite, a nepheline minette-shoshonite suite, and a chemically distinct younger volcanic suite. Petrographic and geochemical data indicate that the intrusive complex and older volcanic suite are largely comagmatic. This relationship is substantiated by similarities in ages and proximity of the older volcanic rocks to the intrusive suite. No significant chemical differences occur between these two suites, except where hydrothermal alteration has increased the concentration of Cu and K in the intrusions at the expense of Na.

The nepheline minette lava flows extruded at ~38 Ma are primitive. They are characterized by Mg # >65, high concentrations of volatiles, LILE, and LREE, and strongly compatible elements. They contain relatively low concentrations of Ti, Nb, and Zr on a mantle-normalized basis, 15 to 18 percent normative nepheline, and 1 to 15 percent normative leucite. The nepheline minette magmas may be primary melts that are products of small degrees of partial melting of metasomatized, lithospheric mantle. Associated shoshonites lack normative nepheline and normative leucite. At comparable SiO_2 contents, the younger volcanic rocks emplaced at ~32 Ma are generally more aluminous and sodic, and less magnesian and potassic than the older volcanic and intrusive suites.

All magmas except the nepheline minette were sulfide-saturated when erupted and contain magmatic sulfides as 1 to 100 micron-diameter elliptical inclusions in mafic mineral phenocrysts. Analytical data suggest that sulfides accommodate most of the Cu and Ag that are present in the magmas. Resorption and oxidation of the sulfides may have made these metals available to the hydrothermal system. The sulfide-undersaturated character of the primitive, alkaline magmas may have allowed them to rise through the crust with almost no loss of S, Cu, and other chalcophile metals.

Fractional crystallization, magma mixing, and assimilation all played roles in determining the composition of the magmas in the Bingham system. Trace-element modeling shows that the minette flows are not related to the other volcanic suites or to the intrusive suite by fractional crystallization. However, mixing of the minette magma with latitic magma could have

created the shoshonites and the magma of the older suite. Trace-element modeling also indicates that late mineralized dikes may be formed by mixing of about 10 percent minette magma and 90 percent calc-alkaline magma. Degassing of mixed minette magma underlying the calc-alkaline magma may have contributed even larger proportions of sulfur, volatiles, and metals to the ore-forming system.

Introduction

The genetic relationship between porphyry copper deposits and their granitic hosts has long been investigated and debated. The orthomagmatic theory, developed by Burnham (1979), suggests that copper is removed from a melt by chlorine-rich aqueous fluids that exsolve under reduced pressure. Cline and Bodnar (1991) propose that a typical calc-alkaline magma contains sufficient copper, chlorine, and water to produce economic porphyry copper mineralization. Candela (1989a) suggests that "volatile constituents" exert strong controls on the quantity, chemistry, and style of mineralization of porphyry deposits. However, he suggests that the presence of magmatic sulfides may lead to the sequestering of copper in solids and a low efficiency of removal by chlorine-bearing fluids (Candela, 1989b).

The Bingham Canyon porphyry Cu-Au-Mo deposit in the central Oquirrh Mountains of Utah (Fig. 1) lies in monzonite, quartz monzonite, and quartz latite intrusions intruded at 39.8 ± 0.4 to 37.5 ± 0.4 Ma into Paleozoic quartzite and limestone (Moore, 1973a; Moore 1973b, Lanier et al., 1978; Warnaars et al., 1978). Some of the igneous rocks vented from 39 to 33 Ma and formed a volcanic pile that is partially preserved on the eastern flank of the Oquirrh Mountains (Smith, 1961; Moore et al., 1968; Moore, 1973b; Lanier et al., 1978; Warnaars et al., 1978; Moore and McKee, 1983; McKee et al., 1993). Small volumes of distinctive, volatile-rich, mafic alkaline magmas also erupted to form nepheline minette lava flows interbedded with the intermediate calc-alkaline volcanic rocks (Gilluly, 1932; Moore, 1973a).

This report summarizes a petrographic and petrochemical study of the igneous rocks of the Bingham mining district and an evaluation of the relationship between copper mineralization and alkalic magmatism. Sample locations and additional data are presented in Waite (1996).

Geologic Setting

The Bingham mining district is located in the Oquirrh Mountains (Figs. 1 and 2), a north-trending, fault-bounded range in the eastern Great Basin that is composed of folded Paleozoic sedimentary rocks cut by thrust, normal, and strike-slip faults (James et al., 1961; Tooker and Roberts, 1961).

The Oquirrh Mountains lie in the western part of the Uinta Axis, an east-west lineament, which has been an intermittently active structural zone since late Precambrian time (Erickson, 1976). Archean cratonic rocks >2.5 Ga are found in isolated outcrops in northern Utah, Idaho, and Wyoming to the north of the Uinta Axis. Link et al. (1993) suggest that early Proterozoic

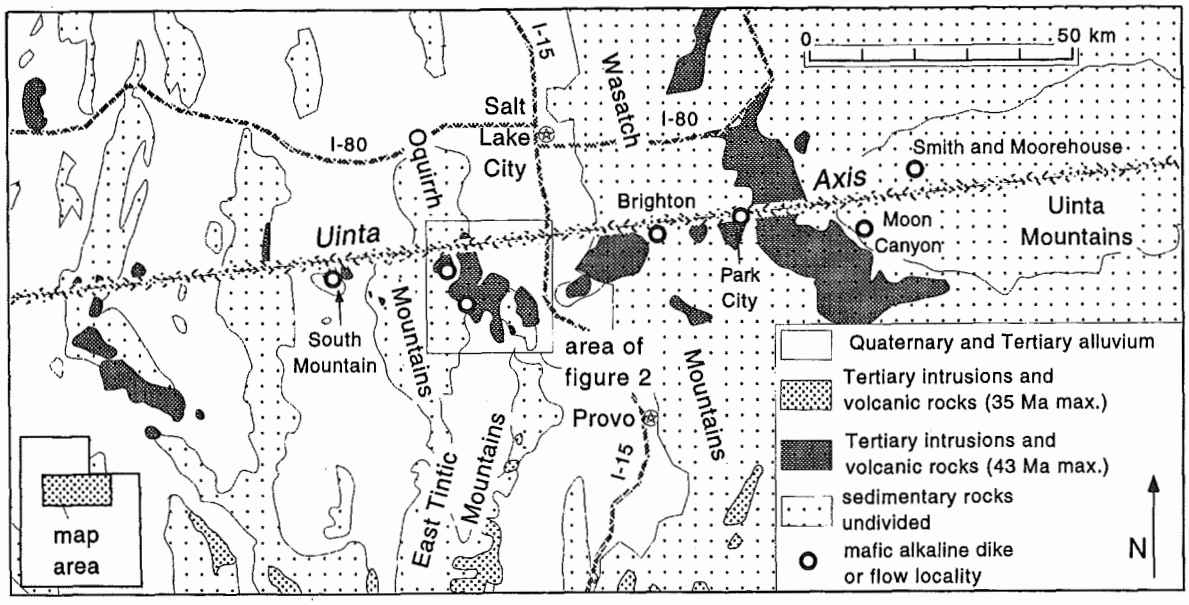

FIG. 1. Index map showing the location of the Bingham district and other features referred to in the text. The dashed line represents the Uinta axis; also known as the Stockton-Park City intrusive belt.

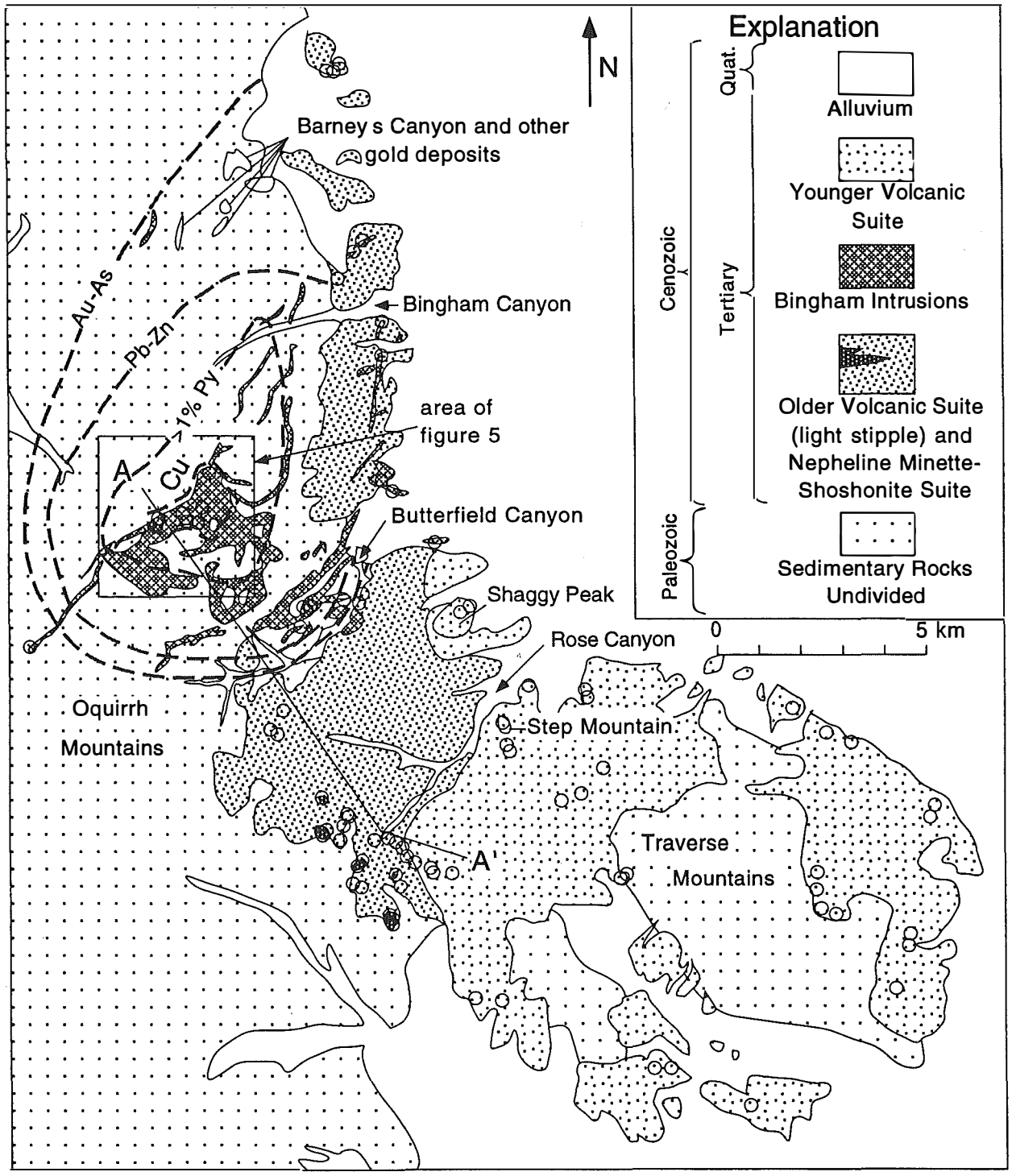

FIG. 2. Simplified geologic map of the west flank of the Oquirrh Mountains, Utah. Small circles represent sample locations. Dashed lines outline the limits of the Bingham Canyon copper orebody and associated mineralized halos as labeled (Babcock et al., 1995). Boundary between older and younger volcanic suites is approximated from the data of this study; other geologic contacts are compiled from Smith (1961) and Babcock et al. (1995).

rocks are accreted to the Archean craton along an approximately east-west suture believed by Helm (1994) to coincide with the Uinta Axis (Fig. 1). This lineament, also known as the Stockton-Park City intrusive belt, is marked by the west-trending Uinta Mountains and a zone of magnetic anomalies (Stewart et al., 1977). Regional aeromagnetic surveys suggest that a large west-trending igneous body underlies the entire Stockton-Park City intrusive belt at depths of a few kilometers (Ballantyne et al., 1995).

Igneous rocks at Bingham were formed as part of a southward sweeping volcanic episode that entered the northern part of the Basin and Range province about 43 Ma (Stewart and Carlson, 1976; Best and Christiansen, 1991). Cross and Pilger (1978), Lipman (1980), and Best and Christiansen (1991) all suggest that the southward sweep of volcanism was related to progressive steepening and foundering of the subducting oceanic lithosphere beneath continental lithosphere. This volcanic episode continued southward along an arcuate east-west front reaching southern Nevada by Miocene time (Best et al., 1989).

Presnell (1992; 1997) suggests that Cenozoic tectonism at Bingham was largely extensional, starting with minor Eocene extension associated with intrusions, dikes, and fissures, and ending with major Miocene-to-Holocene Basin-and-Range extension. Seedorff (1991) suggests that most Tertiary porphyry deposits in the Great Basin are related to the bimodal magmas that were generally emplaced synchronously with, or immediately before, the onset of extension. He contends that the Bingham and Tintic-East Tintic districts were emplaced during a period of rapid extension.

Eocene to Oligocene magmatic activity occurred for 120 km along the Uinta Axis from 20 km west of Bingham to the western Uinta Mountains (Moore and McKee, 1983). Magmatism near the Bingham mining district spanned a period of about 8 m.y. from the latest Eocene to middle Oligocene time.

Volcanic rocks ranging from nepheline minette to rhyolite are well-exposed along a 13-km long, north-south belt on the eastern flank of the east-tilted Oquirrh Mountains. The most complete section is in the western Traverse Mountains (Fig. 2). Debris avalanche and lahar deposits of latitic composition are the most common volcanic rock type and appear to have originated from small domes, shallowly eroded dikes, and minor lava flows.

Within the Bingham mining district, the equigranular monzonite of the Last Chance and Bingham stocks is the oldest intrusive phase (39.8–37.5 Ma), followed by the quartz monzonite porphyry phase of the Bingham stock, then latite porphyry and quartz latite porphyry dikes, and finally the 33.0 Ma Shaggy Peak rhyolite plug (Moore, 1973a; Warnaars et al., 1978).

Sampling and Analytical Techniques

Ninety-one samples of volcanic and intrusive rocks were collected near the Bingham Canyon porphyry deposit and were studied together with four samples collected by Barr (1993). Samples for modal and chemical analyses were neither significantly weathered nor hydrothermally altered. All samples were examined by standard petrographic methods to determine mineral assemblages and textures. A small set of the samples was point-counted to determine modal proportions of the phenocrysts (Waite 1996).

Phenocryst compositions of selected samples were determined by wavelength-dispersive electron microprobe analysis using a JEOL JXA-8600 Superprobe at the University of Georgia. Major- and trace-element analyses were determined for 95 whole-rock samples by X-ray fluorescence methods using a Siemens SRS 303 spectrometer at Brigham Young University. Major-element analyses were determined on fused glass discs prepared with a lanthanum-bearing lithium tetraborate fusion mixture and trace-element analyses were determined using two grams of rock powder pressed into pellets backed with cellulose. Matrix effects were corrected using the Siemens Spectra-AT software concentration I model. Precision and accuracy of the analyses were determined by multiple analysis of international standards.

The concentrations and isotopic ratios of Nd, Sm, Rb, and Sr were determined at the University of Ottawa. Mixed spikes of ^{84}Sr-^{87}Sr, ^{148}Nd-^{149}Sm were added to the samples of 50 mg in Savillex screw-top Teflon vials. The mixtures were dissolved using HF-$HClO_4$ (10:1) at 200°C overnight, followed by drying and reaction with 6 N HCl at 150°C. Rb and Sr were eluted with 2.5 N HCl and REE with 6.1 N HCl using BioRad AG 50 W-X8 (200–400 mesh). Nd and Sm were separated from other REE using a Teflon powder resin coated with di-ethylhexyl orthophosphoric acid. Total chemical blanks are less than <0.1 ng for Nd and <0.05 ng for Sr, negligible in comparison to the minimum amounts of Sr (37,000 ng) and Nd (1,200 ng) in the sample aliquots. Isotopic measurements were made on a multi-collector thermal ionization mass spectrometer (Finnigan MAT 261), and the ratios for Sr and Nd isotopes were normalized to $^{86}Sr/^{88}Sr$ of 0.1194 and $^{146}Nd/^{144}Nd$ of 0.7219. During the course of isotopic analysis (May–June, 1995) measurements of NBS987 and La Jolla gave $^{87}Sr/^{86}Sr$ of 0.7102277 ± 12 (N = 7) and $^{143}Nd/^{144}Nd$ of 0.511855 ± 20 (N = 7).

Field Characteristics

Volcanic rocks near the Bingham Canyon porphyry copper deposit range in composition from nepheline minette lavas to rhyolite domes, but latite breccias are dominant. These rocks and associated intrusive rocks in the Bingham mining district can be divided into four distinct chrono-compositional suites. A younger/older division was recognized by Moore (1973b). We have subdivided the 1-km-thick volcanic sequence into three informal suites: an older volcanic suite, a nepheline minette-shoshonite suite which occurs within the upper part of the older volcanic suite, and a younger volcanic suite. The intrusive suite is treated as a fourth group.

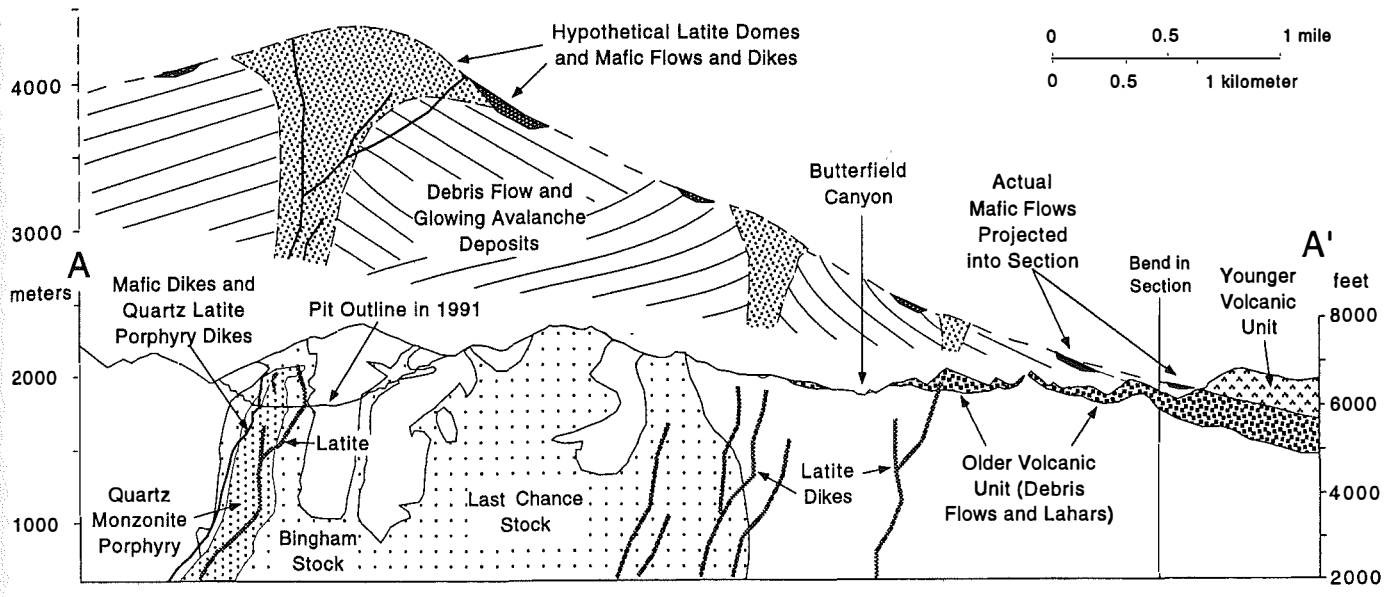

FIG. 3. Cross-section A-A' (Fig. 2) depicting a hypothetical volcanic edifice over the Bingham Canyon porphyry copper deposit. The reconstructed cover infers that some of the Bingham intrusions vented to form domes that decrepitated to form the existing debris avalanche deposits. Note the occurrence of mafic dikes within the pit. Geologic contacts compiled from Babcock et al. (1995) and unpublished Kennecott maps.

Older Volcanic Suite

Older volcanic rocks west of Step Mountain (Fig. 2) were emplaced at about 38.5 Ma and are largely coeval with the Bingham intrusions (Moore and McKee, 1983). In the western Traverse Range, the older volcanic suite covers an area of approximately 6.5 km^2 (Fig. 2) and contains debris flows, ash-flow tuffs, and flow breccias. Gilluly (1932) determined the thickness of this sequence east of Butterfield Canyon to be about 580 m. The breccias consist of subangular to rounded fragments of latite ranging in size from several centimeters to several meters in a matrix of lithic and crystal fragments. Local venting of Bingham porphyritic magmas likely fed latitic domes and debris avalanches. Extrapolation of the Tertiary-Paleozoic contact suggests that this volcanic suite, or its parental domes, may have been present less than 500 m above the pre-mining surface of the deposit (Fig. 3).

Nepheline Minette-Shoshonite Suite

Nepheline minette and shoshonitic lava flows emplaced at 37.7 Ma (McKee et al., 1993) are intercalated within the upper part of the older volcanic suite (Fig. 2). The contacts of the nepheline minette and shoshonite are poorly exposed. Narrow dikes of similar composition have recently been found in the Bingham pit.

Figure 4 shows that most mafic lava samples collected are basanites according to the IUGS chemical classification scheme (Le Maitre, 1989); however, because they contain phlogopite phenocrysts, nepheline, and felsic minerals in the groundmass, we classify these rocks as nepheline minettes following the terminology of Wallace and Carmichael (1989).

Younger Volcanic Suite

The volcanic rocks east of Step Mountain are generally more silicic and comprise the younger volcanic rock suite. The chemical composition of the younger suite is similar in many respects to the Bingham intrusions, but important differences do exist. Several K-Ar ages show that the younger suite is several m.y. younger than both the Bingham intrusions and the older volcanic suite Moore (1973a). For example, the rhyolite vitrophyre and the latite tuff breccia in the Traverse Mountains (Fig. 2) have ages of 31.2 Ma and 30.7 Ma, respectively (Moore, 1973a).

The younger volcanic suite in the western Traverse Range is comprised of lava flows, minor ash-flow tuffs, and subordinate breccias that are as much as 300 m thick and cover an area of approximately 9 km^2 (Gilluly, 1932; Moore, 1973b; Fig. 3). Light gray, porphyritic, flow-layered andesite and dacite lava flows predominate over pyroclastic units. Some flows contain inclusions of Oquirrh Group quartzite. Breccias in the younger suite are similar to those in the older suite except for the presence of tuff fragments. East of Rose Canyon, outcrops of a monolithic latite tuff breccia are preserved. This distinctive tuff breccia has a minimum thickness of approximately 180 m (Moore, 1973a) and has been dated at 30.7 Ma (Moore et al., 1968).

The tuff breccias are overlain by a series of latite and perlitic, rhyolite vitrophyre autobreccias which are flow-layered in colors of green, pink and tan and contain phenocrysts of plagioclase and small biotite flakes. Moore et al. (1968) reported a K-Ar age of 31.2 Ma for a rhyolite vitrophyre.

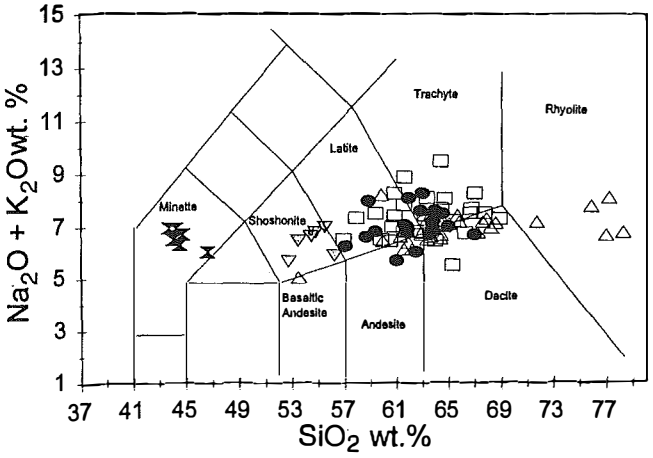

FIG. 4. IUGS classification (Le Maitre, 1989) scheme for Bingham intrusive and extrusive rocks. Data shown for Bingham samples: younger volcanic unit (*open triangles*), older volcanic unit (*stippled ellipses*), nepheline minette (*solid hourglasses*), shoshonite (*stippled inverted tirangles*), and intrusive unit (*open squares*).

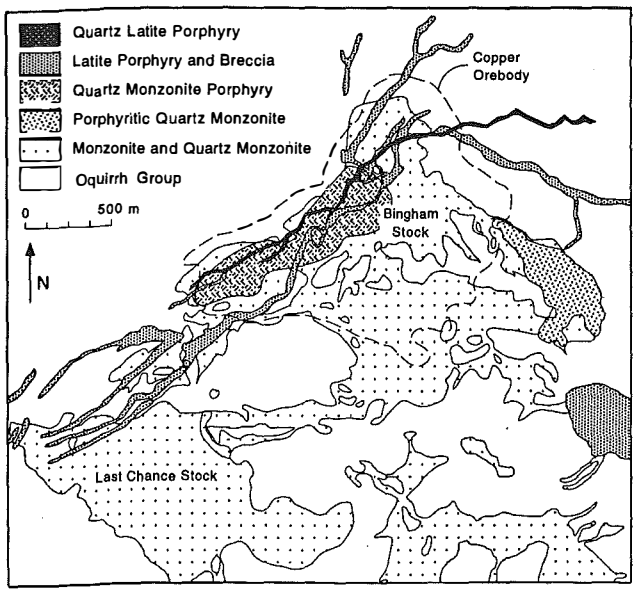

FIG. 5. Simplified geologic map of the Bingham mine area. Geologic contacts are compiled from unpublished Kennecott maps.

Intrusive Suite

The four principal intrusive rock types found in the Bingham mining district are shown in Figure 5. The intrusive suite represented from oldest to youngest (Lanier et al., 1978) consists of: (1) Monzonite: the most common rock type exposed in the Bingham stock and an important host rock for porphyry copper ore, (2) Quartz monzonite porphyry: the major porphyry intrusion in the Bingham stock and an important ore host, (3) Latite porphyry: dikes and sills that intrude the Bingham stock, (4) Quartz latite porphyry: narrow dikes, less than 10 m wide, that intrude all of the other rock types.

The equigranular Last Chance stock and the equigranular portion of the Bingham stock are interconnected and were passively emplaced by stoping and assimilation (Willden, 1952; Moore, 1973a), whereas porphyritic phases of the Bingham stock were forcefully intruded (Bray, 1969). The Bingham stock and the northwestern part of the Last Chance stock are intruded by narrow latite and quartz latite porphyry dikes. These intrusions contain phenocrysts of plagioclase, biotite, and hornblende in a dark-gray cryptocrystalline groundmass. Within the mine area, the dikes are altered, but they are less intensely fractured and mineralized than the monzonite and quartz monzonite porphyry phases of the Bingham stock. We concur with Moore's (1973a) suggestion that, of all the Bingham intrusions, the amphibole-bearing latite dikes most closely match the composition of some volcanic rock types in the volcanic sequence.

Unmineralized intrusions occur in several locations in the Bingham mining district (Fig. 2). The 33.0 Ma (Moore, 1973a) Shaggy Peak plug is composed of dark gray vitrophyric rhyolite. Steeply dipping flow structures and sheeting show that the rhyolite intruded the surrounding latite flows. Step Mountain, another oval plug or dome, has pronounced columnar joints.

The Bingham deposit exhibits strongly concentric zoning of sulfide mineralogy (Fig. 2) and sulfide mineral abundances (John, 1978; Phillips et al., 1997). Warnaars et al. (1978) suggest that mineralization at Bingham most likely took place during several pulses or episodes of hydrothermal activity that started after the intrusion of the equigranular monzonite (39.8 ± 0.4 Ma). Mineralization most likely occurred during and before the emplacement of the quartz latite porphyry, which is weakly fractured and less altered than its wall rocks.

Petrographic and Chemical Characteristics

Most of the Bingham rocks have porphyritic to microporphyritic textures and glassy to microcrystalline groundmasses. Common phenocrysts include olivine, clinopyroxene, orthopyroxene, plagioclase, biotite, amphibole, and Fe-Ti oxides (mostly magnetite with minor ilmenite). Glomerocrysts of clinopyroxene, biotite, magnetite, and plagioclase are common. Olivine occurs only in the nepheline minette and shoshonite. Quartz and K-feldspar phenocrysts are prominent in the rhyolite

flows and plugs, and in the Bingham and Last Chance stocks. Apatite occurs as microphenocrysts in all samples. Trace amounts of magmatic sulfides are evident in the freshest volcanic rocks and unaltered intrusive rocks. However, the nepheline minette is not sulfide-saturated.

Whole-rock major and trace element analyses for 20 representative rocks are presented in Table 1. Bingham igneous rocks range from minette to rhyolite (44–78 wt % SiO_2; Fig. 5). Volcanic rock nomenclature is applied to both the volcanic and hypabyssal intrusive rocks because the latter have fine-grained groundmasses and to simplify comparison of the extrusive and intrusive rocks.

Older Volcanic Suite

The proximity of the older volcanic rocks and the intrusive suite, along with their chemical similarities, as shown on variation diagrams (Figs. 6 and 7), suggest that the two are coeval. Most of the variation diagrams, show no significant differences between the two suites over the observed range of SiO_2 (52–69 wt %). Obvious exceptions to this generalization are noted in Cu and K where hydrothermal alteration has increased their concentration in the intrusions.

Major-element variation diagrams (Fig. 6) show smooth linear decreases in the concentrations of all major elements except K, Na, and Al relative to increase in silica content. Al shows initial enrichment and then a decrease with increasing silica. Trace-element variation diagrams (Fig. 7) show generally progressive decreasing concentrations of Ba and Sr with increasing SiO_2. The lavas are all strongly enriched in light rare earth elements (LREE) when abundances are normalized to chondritic values (Fig. 8). High concentrations of large ion lithophile elements (LILE) compared with high field strength elements (HFSE) ($50 < Ba/Nb < 250$) suggest a contribution from subduction processes (Ormerod et al., 1988). Most of the Bingham samples have Ba/Nb within the range of 50 to 250 (Fig. 9). The older volcanic suite has higher Ba/Nb ratios than the younger volcanic suite.

Nepheline Minette-Shoshonite Suite

All nepheline minette samples contain olivine (Fo_{85-92}) and phlogopite phenocrysts, 15 to 18 percent normative nepheline, and 1 to 15 percent normative leucite (Table 1). They are silica-undersaturated and have high concentrations of incompatible elements. Chondrite-normalized trace-element diagrams show an enrichment in LILE and deep troughs at Nb and Ti (Fig. 8), as is typical of subduction-related rocks. However, the nepheline minettes are Ne-normative and have high Mg # [$Mg\ \# = 100 * (Mg / Mg + 0.80\ Fe^{+2})$], and high Mg, Ni, and Cr, which is more characteristic of continental rifts such as the Rhine Graben and East Africa rift, or intraplate hot spots (Perfit, 1985).

The presence of Mg-rich olivine and phlogopite phenocrysts provides good evidence that the nepheline minettes are derived from an olivine-phlogopite-bearing source. This, and other chemical characteristics suggest that the nepheline minettes are primary melts and products of small-degree partial melting of the mantle that erupted without significant differentiation (Green, 1970). A plot of Ni versus Mg # (Fig. 10) shows comparison with a primary magma field (Mitchell and Platt, 1984). All but one of the nepheline minette samples and two of the shoshonite samples fall within the field. Assigning Mg numbers to highly oxidized, water-rich magmas like those at Bingham is difficult because of the strong dependence of the Mg # on the oxidation state of the magma. The use of Mg # in classifying basic magma is dependent upon the oxidation state of the magma; the higher the assumed ferric iron content, the higher the calculated Mg #. For the Bingham rocks, we have assumed Fe^{+3} = 20 percent of total Fe. For $Fe^{+3} > 20$ percent, the resulting Mg #s are very high, suggesting fractionation and accumulation of olivine.

The shoshonites contain more silica than the nepheline minettes, but do not exceed 56.5 percent SiO_2. They do not contain normative nepheline or leucite. Both rock types contain abundant large olivine phenocrysts and smaller clinopyroxene phenocrysts, and the nepheline minette also contains oxidized biotite or phlogopite.

Intrusive Suite

All the intrusive rock samples exhibit similar compositional trends. Ca and Fe contents decrease with increasing silica, whereas Al, K, and P concentrations remain constant over the range of SiO_2. Trace elements, such as Ce and Zr, show scatter over the same range of SiO_2 (Figs. 6 and 7).

Younger Volcanic Suite

The younger volcanic suite is chemically distinctive from the other suites. Except for the rhyolite, the entire younger suite is generally enriched in Al, K, and Na and depleted in Mg compared to the intrusive and older volcanic suites. At comparable SiO_2, the lavas of the younger suite contain more TiO_2 than the other suites.

The younger suite generally contains higher concentrations of Nb than the other suites, but rhyolite samples have Nb contents similar to the nepheline minettes (Fig. 7). Rb contents of the nepheline minettes, shoshonites, and the younger suite are similar, and are lower than in the other suites (Fig. 7). Ba/Nb ratios for the younger suite are consistently lower than for the other suites (Fig. 9).

Mineralogy

Feldspar. Feldspar phenocrysts show a wide range in composition: anorthoclase in the shoshonite suite, labradorite in the older volcanic suite, andesine in the younger volcanic suite and in a latite porphyry dike, and oligoclase in the Last Chance stock. Feldspars from all of the suites show considerable zoning in both the normal and reverse sense.

Clinopyroxene. Clinopyroxene in most Bingham mining district rocks is weakly zoned, and commonly exhibits

TABLE 1. Major- and trace-element concentrations from samples collected in the Bingham District

Sample #	Tick-1	Tick-2	Tick-16A	Tick-17	Tick-21	Tick-33	Tick-37	Tick-38	Tick-39	Tick-43	Tick-44	Tick-44A	Tick-46	Tick-48	Jord-12	Bing-6	Bing-12	Bing-19	Lowe-3	Lark-2
Rock unit::	NM	NM	S	Y	Y	O	NM	NM	NM	NM	NM	S	S	S	Y	I	I	I	O	O
Rock Type:	Minette	Minette	Shoshonite	Trachyte	Trachyte	Latite	Minette	Minette	Minette	Minette	Minette	Shoshonite	Shoshonite	Shoshonite	Andesite	Latite	Dcaite	Monzonite	Latite	Andesite
Major																				
SiO_2	45.69	44.73	52.71	63.80	63.71	59.36	444.03	43.70	44.16	44.21	44.54	56.18	58.60	55.57	61.54	61.54	62.89	57.88	64.51	62.45
TiO_2	0.99	0.99	1.24	0.78	0.83	0.82	0.87	0.86	0.87	0.89	0.88	0.71	0.67	0.97	0.89	0.69	0.69	0.99	0.67	0.86
Al_2O_3	10.33	10.37	15.43	16.25	16.17	14.36	10.18	10.15	10.20	10.31	10.38	12.38	13.05	13.24	16.80	14.81	14.50	15.20	17.02	15.62
Fe_2O_3*total	11.32	10.91	8.91	5.08	5.52	7.11	11.69	11.79	11.53	11.42	11.57	7.76	7.13	6.72	5.94	6.19	6.10	7.29	4.25	5.59
MnO	0.20	0.18	0.14	0.08	0.08	0.11	0.20	0.19	0.20	0.20	0.20	0.13	0.10	0.09	0.10	0.09	0.09	0.11	0.09	0.09
MgO	13.43	14.98	6.39	2.10	2.05	4.98	15.61	15.42	15.46	15.00	15.21	9.40	7.84	6.38	2.97	4.23	4.23	4.38	1.56	3.71
CaO	10.91	10.68	8.96	4.09	4.14	6.01	10.44	10.56	10.51	10.65	10.45	7.16	5.60	9.39	5.18	5.31	4.49	6.31	4.04	5.35
Na_2O	3.27	3.84	3.01	3.46	3.62	3.09	3.27	3.68	3.37	3.87	3.37	2.25	2.30	3.36	3.10	3.14	2.98	3.38	3.25	2.54
K_2O	2.75	2.88	2.67	3.93	3.56	3.75	3.23	3.26	3.18	3.07	2.95	3.66	4.32	3.73	3.04	3.67	3.74	3.96	4.27	3.51
P_2O_5	0.21	0.45	0.55	0.42	0.33	0.41	0.48	0.39	0.52	0.38	0.45	0.36	0.38	0.56	0.43	0.34	0.32	0.49	0.35	0.30
Sum	100.00	100.01	100.01	99.99	100.01	100.00	100.00	100.00	100.00	100.00	100.00	99.99	99.99	100.01	99.99	100.01	100.02	99.99	100.01	100.02
Anal. Total	99.63	67.67	97.95	100.21	100.47	99.25	97.26	97.05	97.29	97.44	98.33	100.72	100.67	98.62	99.12	99.86	100.18	98.59	98.83	99.39
LOI	2.01	1.40	0.87	1.92	1.72	1.19	2.28	1.83	2.25	2.06	2.48	1.29	1.16	1.38	1.99	1.30	2.37	0.35	1.77	1.89
MG#	71.33	74.22	60.06	46.43	43.78	59.49	73.68	73.28	73.76	73.36	73.38	71.75	69.75	66.56	51.18	58.90	59.25	55.75	43.49	58.19
ppm																				
F	4482	5451	626	924	552	497	2771	3070	2855	3368	3296	333	525	1812	553	590	1146	740	570	387
S	56	20	349	74	44	217	0	0	0	0	0	0	0	2351	235	118	8500	113	143	81
Cl	60	172	270	315	346	320	1.24	82	88	86	64	287	290	122	179	191	80	457	273	195
Sc	19	24	24	6	7	16	23	21	21	22	21	17	15	20	9	16	9	12	6	12
V	153	192	285	81	100	152	158	145	154	148	170	144	128	193	113	142	130	161	117	146
Cr	1294	880	132	0	1	217	1157	1146	1152	1201	1167	689	583	442	28	166	853	28	0	58
Ni	392	323	43	14	11	58	356	352	362	349	346	328	257	59	24	52	45	31	0	52
Cu	125	108	53	19	21	22	91	99	101	95	93	54	60	63	31	36	369	43	12	33
Zn	96	95	86	72	73	77	86	84	84	84	85	76	74	67	77	72	74	84	116	78
Ga	13	13	20	23	21	20	14	14	14	14	14	19	19	18	22	18	21	23	2	21
Rb	105	78	57	122	110	106	113	102	95	85	87	102	129	102	79	105	216	105	137	104
Sr	863	1178	1668	832	651	787	907	846	1105	752	1258	756	737	814	677	708	203	1199	933	756
Y	26	24	31	23	24	21	24	24	24	24	24	19	19	27	21	20	15	20	20	19
Zr	149	125	205	259	249	252	127	121	122	121	124	214	218	188	247	229	228	219	312	266
Nb	28	23	10	19	18	11	23	23	22	23	23	9	8	13	17	13	16	9	14	12
Ba	4439	3165	3375	1805	1581	2131	2332	2236	2284	1700	2749	1728	1859	2449	1543	2074	2100	2518	2140	1812
La	55	70	156	101	78	83	84	79	77	69	75	88	89	85	69	76	99	92	103	86
Ce	105	85	281	168	147	125	91	84	87	84	85	121	116	124	133	117	152	159	177	148
Nd	57	49	118	73	61	50	46	47	43	47	47	41	40	46	55	47	54	62	60	48
Sm	2	9	17	13	11	10	11	11	10	10	9	10	10	10	9	10	12	12	11	9
Pb	19	13	53	33	27	37	18	14	12	13	13	37	41	26	32	34	61	43	41	32
Th	5	6	30	31	27	19	4	3	4	4	4	11	13	14	23	6	46	20	31	25
U	3	0	6	7	8	4	0	0	0	2	0	0	0	4	6	4	4	6	10	5
CIPW norms																				
Quartz	0.00	0.00	0.00	16.08	16.15	7.74	0.00	0.00	0.00	0.00	0.00	1.74	5.77	0.00	15.29	11.82	14.84	3.93	17.66	16.78
Corundum	0.00	0.00	0.00	0.00	0.00	0.00	0.00	0.00	0.00	0.00	0.00	0.00	0.00	0.00	0.05	0.00	0.00	0.00	0.55	0.00
Orthoclase	14.26	0.00	15.88	23.32	21.12	22.28	0.00	0.00	0.00	0.00	0.99	21.76	25.67	22.15	18.05	21.79	22.14	23.46	25.61	20.83
Albite	0.00	0.00	25.64	29.39	30.76	26.29	0.00	0.00	0.00	0.00	0.00	19.15	19.57	28.57	26.35	26.69	25.33	28.68	27.59	21.58
Anorthite	5.44	2.58	20.85	17.28	17.44	14.32	3.60	1.57	3.35	1.72	4.53	12.96	12.60	10.09	23.00	15.56	15.25	14.66	17.81	20.95
Leucite	1.67	13.46	0.00	0.00	0.00	0.00	15.10	15.24	14.87	14.35	13.01	0.00	0.00	0.00	0.00	0.00	0.00	0.00	0.00	0.00
Nepheline	15.12	17.75	0.00	0.00	0.00	0.00	15.12	17.02	15.58	17.90	15.59	0.00	0.00	0.00	0.00	0.00	0.00	0.00	0.00	0.00
Diopside	38.27	37.82	16.41	0.28	0.86	10.51	32.75	30.67	33.80	34.15	35.83	16.34	10.30	26.55	0.00	7.04	4.08	10.98	0.00	3.03
Hypersthene	0.00	0.00	10.80	9.48	9.47	13.94	0.00	0.00	0.00	0.00	0.00	23.23	21.52	24.22	12.59	12.91	14.25	12.82	7.57	12.62
Olivine	19.03	21.60	0.00	0.00	0.00	0.00	25.28	25.74	24.52	23.46	23.40	0.00	0.00	4.79	0.00	0.00	0.00	0.00	0.00	0.00
Magnetite	3.824	3.684	3.004	1.708	1.856	2.394	3.950	3.984	3.896	3.858	3.909	2.615	2.401	2.262	1.999	2.083	2.052	2.448	1.428	1.880
Ilmenite	1.897	1.896	2.371	1.487	1.583	1.566	1.667	1.648	1.667	1.705	1.686	1.357	1.280	1.852	1.698	1.317	1.316	1.885	1.276	1.640
Apatite	0.488	1.045	1.276	0.971	0.763	0.950	1.116	0.907	1.209	0.883	1.046	0.834	0.880	1.297	0.995	0.787	0.740	1.132	0.809	0.694

Major elements normalized to 100% NM=Nepheline minette unit; S = Shoshonite unit; O = Older volcanic unit; Y = Younger volcanic unit; I = Intrusive unit

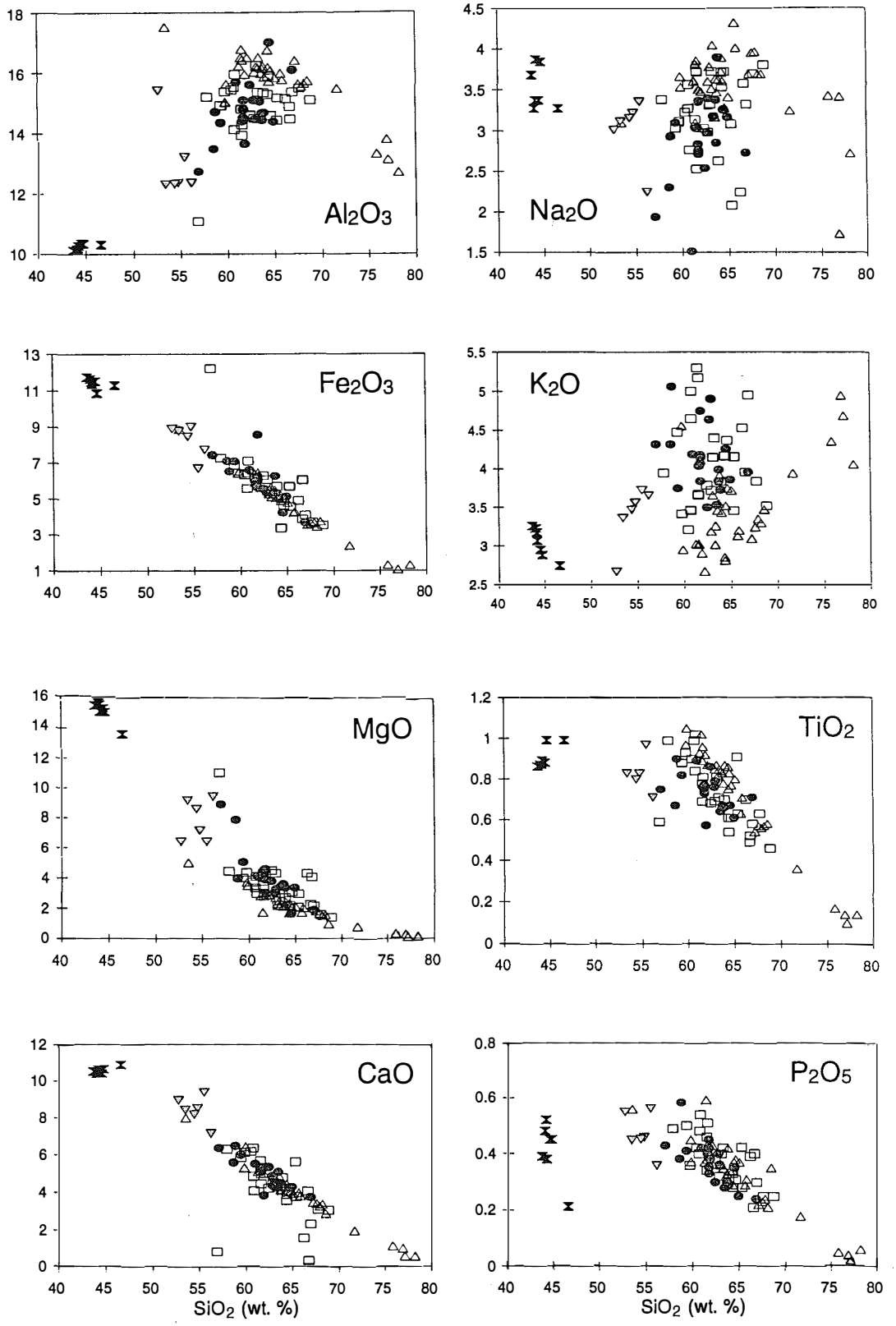

FIG. 6. Major element Harker variation diagrams for Bingham rock samples: younger volcanic unit (*open triangles*), older volcanic unit (*gray ellipses*), nepheline minette (*solid hourglasses*), shoshonite (*gray inverted triangles*), and intrusive unit (*open squares*).

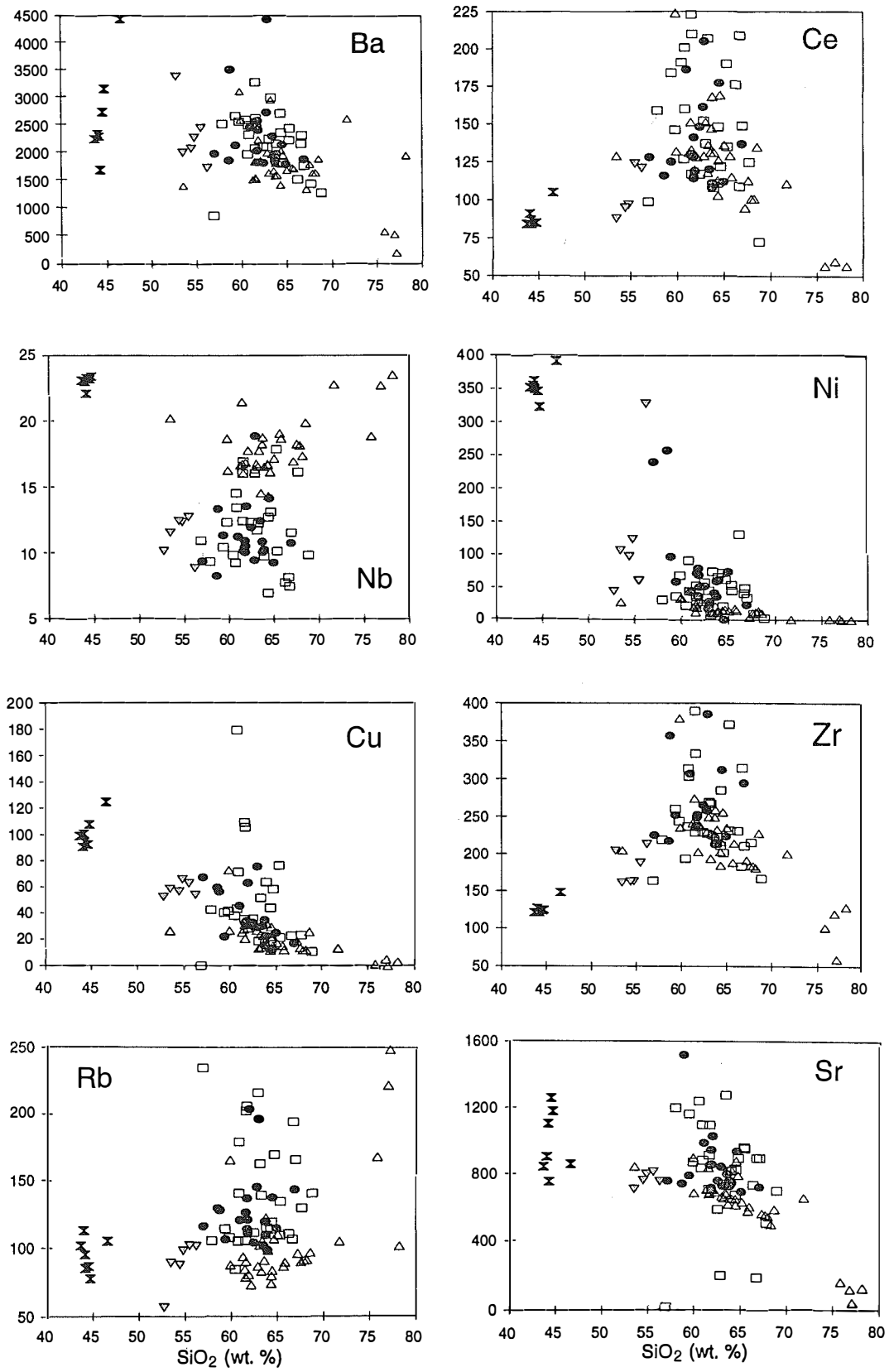

FIG. 7. Harker variation diagrams for trace element components of Bingham igneous suites. Symbols as for Fig. 6.

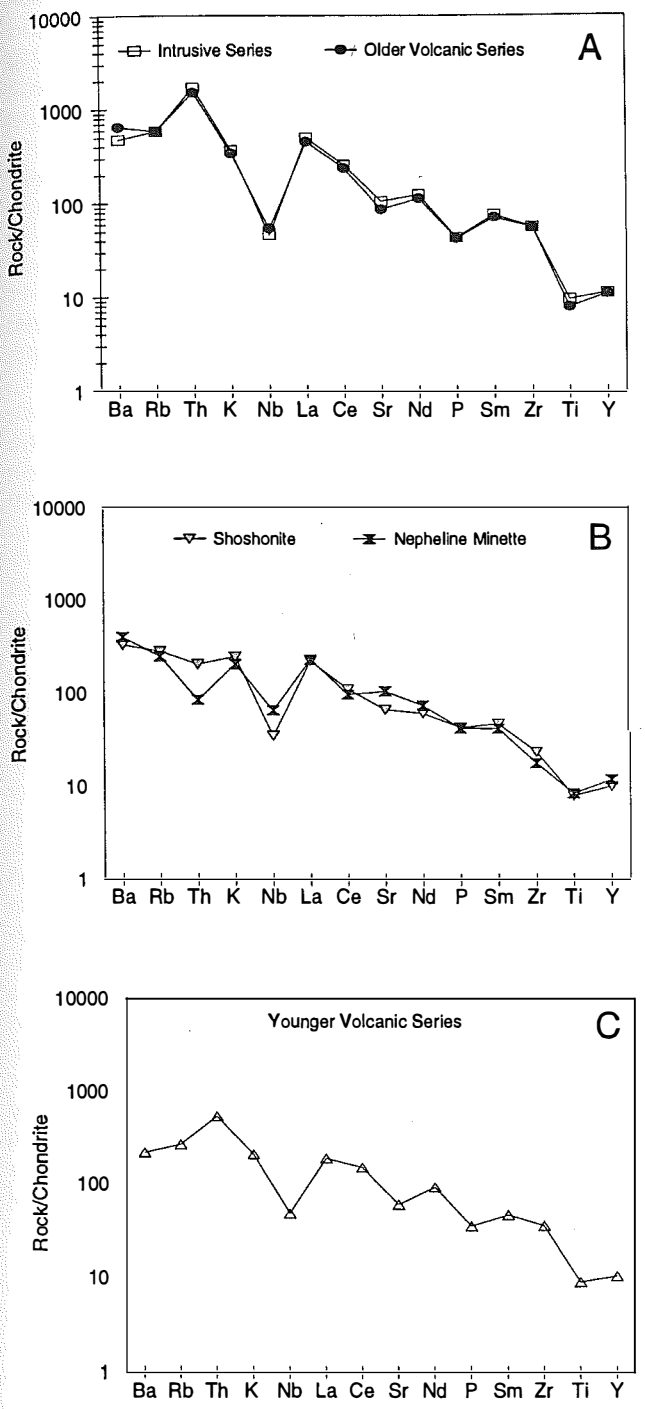

FIG. 8. A) Chondrite-normalized trace-element diagram (Thompson et al., 1984) comparing the older volcanic rocks and the intrusive rocks. The older volcanic rocks fall within the range of the intrusions, which suggests they came from the same magmas. B) Chondrite-normalized diagram comparing the nepheline minette and shoshonite. C) Chondrite-normalized diagram of the younger volcanic series.

simple or lamellar twins. Clinopyroxene (augite) from the older volcanic, younger volcanic, and intrusive suites range in composition from $Wo_{37}En_{55}Fs_8$ to $Wo_{45}En_{42}Fs_{13}$. Clinopyroxene from the nepheline minette is a more calcic diopside, ranging from $Wo_{46}En_{46}Fs_8$ to $Wo_{55}En_{38}Fs_7$ and has the highest Ti content. Several diopside phenocrysts from a nepheline minette sample (Tick 43) have diopside cores with augite rims. Clinopyroxene in the Last Chance Stock is more calcic than in either the older (Tick 33; latite) or younger volcanic suites (Tick 17; trachyte). Clinopyroxene in the younger volcanic suite is unzoned, whereas clinopyroxene from the older volcanic suite is strongly zoned. Moreover, the Mg content of clinopyroxene in the younger volcanic suite is lower than in the nepheline minette, intrusive, and older volcanic suites.

Orthopyroxene. Compositions for orthopyroxene from two younger volcanic samples (Tick 17 and Tick 21) and one older volcanic sample (Tick 33) range from $Wo_5En_{78}Fs_{17}$ to $Wo_2En_{64}Fs_{34}$. Orthopyroxene from the analyzed samples of the younger volcanic suite has more Fe and less Mg than orthopyroxene from the older volcanic suite. Orthopyroxene phenocrysts from the younger suite fall into two distinct groups with respect to Fe/Mg ratios. Orthopyroxene phenocrysts in Tick 17 (trachyte; younger suite) are enriched in Ca, Ti, Al and depleted in Mn relative to Tick 21 (trachyte; younger suite). Orthopyroxene in the younger volcanic suite contains very little Cr (0.0–0.07 wt %) compared to the orthopyroxene in the older volcanic suite (0.24–0.54 wt %).

Biotite. Biotite is found in all suites and forms euhedral to resorbed phenocrysts and microphenocrysts. Magnetite inclusions and magnetite surrounding some biotite phenocrysts reflect oxidation and resorption of the biotite. All of the analyzed biotite is Mg-rich, with the mica in the nepheline minette being more phlogopitic than mica in the other suites.

Amphibole. A euhedral, bladed form is the most common morphology of amphibole, present in most suites except for the nepheline minette. Some phenocrysts are simply twinned and some are strongly zoned. Different degrees of resorption and alteration are shown by ragged rims, and by chlorite replacement in some samples. Amphibole from the Bingham rocks ranges in composition from hastingsite to hornblende.

Olivine. Phenocrysts and microphenocrysts of olivine are abundant in the nepheline minette and shoshonite suites. Bingham olivine exhibits several distinct morphologies: the two most common are large equant crystals and smaller skeletal crystals. Lofgren (1980) showed that variations in olivine morphology from a euhedral phenocryst to a non-equilibrium skeletal growth form commonly reflect an increase in the cooling rate or substantial undercooling during growth. Olivine from the Bingham nepheline minette is relatively homogeneous, but slight normal zoning is present. The olivine is highly magnesian with com-

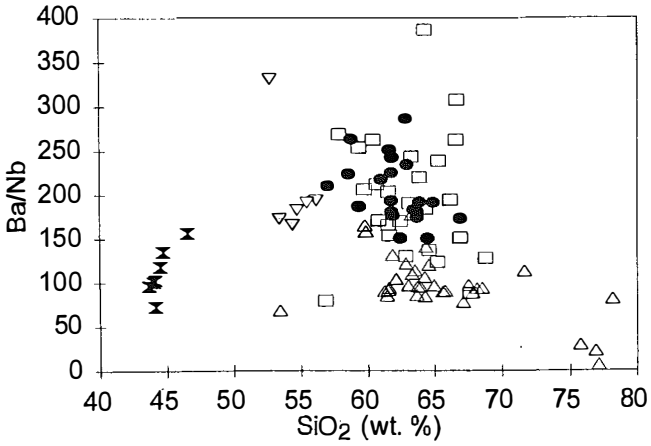

FIG. 9. Ba/Nb ratios versus SiO_2. High concentrations of large ion lithophile elements (LILE) compared with high field strength element (HFSE) (50 < Ba/Nb < 250) probably reflect a contribution from subduction processes (Ormeroid et al., 1988). Most of the Bingham samples have Ba/Nb within the range of 50–250. The older volcanic suite has higher Ba/Nb ratios than the younger volcanic suite.

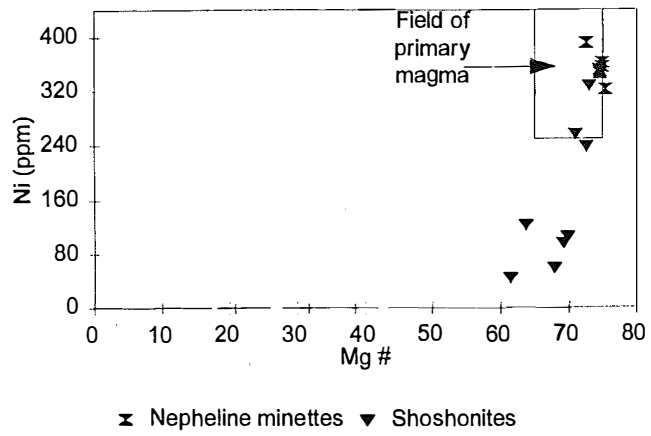

FIG. 10. Field for primitive magmas derived from melting of mantle peridotite is based upon the criteria of Sato (1977) and Green (1971).

positions of Fo_{85-92}, which is close to the range (Fo_{88-94}) expected for primitive magmas derived from "normal" mantle (Basaltic Volcanism Study Project, 1981) and near the range (Fo_{87-94}) in phlogopite-bearing mantle inclusions (Erlank et al., 1987).

Sulfide minerals. Several lines of evidence suggest that a suite of sulfide minerals that occur as inclusions within mafic phenocrysts are magmatic in origin. Magmatic sulfide inclusions are typically present in samples of the older volcanic suite, the younger volcanic suite, the shoshonite flows, and the least-altered intrusions; no magmatic sulfides were observed in the nepheline minette flows.

The sulfide inclusions typically have rounded shapes and are less than 20 microns in diameter. Inclusion relationships indicate that immiscible Fe-Ni-Cu sulfide liquid or solid blebs formed near the surfaces of growing Fe-Mg phenocrysts. The most common hosts for the sulfide inclusions are Fe-rich phases; they are less common in plagioclase, biotite, and the groundmass.

Study of 15 samples containing sulfide inclusions indicates that all suites include both Fe-sulfide in the monosulfide solution (mss) field of the Cu-Fe-Ni-S system and Fe-Cu sulfide in the intermediate solid solution (iss) field (Craig and Kullerud, 1969; Craig and Scott, 1974). Other preserved sulfide minerals include abundant pyrrhotite, chalcopyrite, pentlandite, and rare pyrite, hazelwoodite, millerite, bornite, and chalcocite (Hook, 1995).

Evidence of severe sulfide inclusion degassing (oxidation) and resorption is commonly found, making determination of the original magmatic sulfide abundance problematic, but it is estimated that most samples have between 0.01 and 0.001 volume percent sulfides (Hook, 1995).

Some chemical distinctions are apparent between sulfide inclusions from the different lithologic suites. For example, magmatic sulfide minerals from the older suite are distinctly more Ni-rich (up to 2.38 wt % in pyrrhotite) than sulfide minerals from the younger suite (0.36 wt % in pyrrhotite; Hook, 1995). This mirrors much higher Ni concentrations in whole rock samples of the older suite versus the younger suite.

The location and composition of some sulfide blebs in the shoshonite flows suggest post-magmatic sulfidation of Fe-Mg silicates by S-rich vapors. This type of inclusion is found along fractures in olivine and clinopyroxene. A vapor-phase origin is suggested by the Co-rich nature of the mss (up to 0.58 wt % Co) and pendlandite (9.60–12.60 wt % Co). Stone et al. (1989) suggest that Co is concentrated in a vapor phase relative to a sulfide liquid or a silicate liquid, and that Co-rich sulfides indicate vapor-phase sulfidation of silicates. Sulfidation of Fe-Mg silicates by a S-Co-rich vapor probably occurred during or after eruption. Continued loss of sulfur from the erupted magma by degassing may be responsible for the resorbed morphology of all sulfides in the shoshonite flow. Other Co-poor sulfide inclusions hosted by growth zones of clinopyroxene indicate that the shoshonite magma also became saturated with a sulfide liquid prior to eruption.

Although the nepheline minette shows no evidence of magmatic sulfide saturation, a few one-micron diameter blebs line vesicles suggesting vapor-phase crystallization of sulfides. The lack of magmatic sulfide inclusions does not indicate that the nepheline minette magma was sulfur-poor, because oxidized, mafic, alkaline magmas may contain large amounts of sulfur (2,000–4,000 ppm) without becoming saturated with sulfide minerals (Carmichael and Ghiorso, 1986). Work in progress (D. Tomlinson, 1996, unpublished data) suggests that the oxygen fugacity of the nepheline minette is just below the magnetite-hematite buffer. This implies that oxidized sulfur species would be far more abundant than reduced sulfur in the minette magma.

Radiogenic Isotope Geochemistry

Sr and Nd isotope ratios for a Bingham latite dike, a sample from the Last Chance stock, a nepheline minette flow, and a shoshonite flow, as well as for two samples from the East Tintic volcanic field, are presented in Table 2 and plotted on Figure 11. Isotopic ratios for the nepheline minette flow fall within the field for younger minette dikes from the nearby Wasatch Plateau and also lie along the trend of values for primitive minettes from Highwood, Montana.

O'Brien et al. (1991) interpreted a well-defined mixing trend for Nd-Sr isotope data from Highwood, Montana (Fig. 1), as indicating that primitive minette magmas were formed by variable mixtures of metasomatized lithospheric mantle and relatively undepleted asthenospheric mantle. In this model, the previously depleted subcontinental mantle lithosphere was modified by an ancient subduction-related event that occurred about 1.9 Ga, creating a Rb-LREE-enriched and U-Th-depleted mantle. Tingey et al. (1991) proposed a similar model for Wasatch Plateau minette dikes, and the compositions of the primitive Bingham nepheline minette flows also suggest essentially the same model. Assuming a depleted mantle, the Nd model age for the Bingham primitive nepheline minette flow is 1.8 Ga (Table 2). If the minette magma was derived from subcontinental mantle, the Nd model age is consistent with crustal formation ages that suggest that this area is underlain by Proterozoic lithosphere.

The Sr and Nd isotope ratios for the Last Chance stock are similar to those determined by Farmer and DePaolo (1983) and Vogel et al. (1997) for other granites in the Oquirrh and Wasatch Mountains. The Sr isotope composition of the Last Chance stock differs widely from the compositions of the late latite dikes and shoshonite flows of the older volcanic suite (Fig. 11). However, isotopic ratios of the latite and shoshonite are similar to other mid-Cenozoic intermediate and silicic volcanic rocks and granites of the eastern Great Basin (E.H. Christiansen, unpub. data; Farmer and DePaolo, 1983, Gans et al., 1989; Grunder and Feeley, 1989).

Petrogenesis

Petrochemical data suggest the intermediate and mafic flows of the older volcanic suite were comagmatic or commingled within the same magma chamber, or system of chambers, that fed the Bingham intrusions. This conclusion is supported, in part, by their spatial proximity (Fig. 2) and by their indistinguishable K-Ar ages (39.8–37.5 Ma for the intrusions and 38.5–37.7 Ma for the mafic flows and older volcanics). Several chemical and modal characteristics are similar for the nepheline minette, shoshonite, the older volcanic suite, and the intrusive suite. However, based on a very few analyses, the volcanic and intrusive suites have different isotopic compositions, and thus are not related by any closed system process.

TABLE 2. Isotope data for whole-rock samples from Bingham and Tintic districts

Sample:	Bing-6	Bing-19	Tick-43	Tick-44A	TD-55	ET-134
Rb ppm	121.60	121.70	61.32	125.30	102.10	133.80
Sr ppm	740.7	1349.4	445.3	815.1	785.4	619.4
$^{87}Rb/^{86}Sr$	0.47518	0.26096	0.39839	0.44504	0.37624	0.62530
$^{87}Sr/^{86}Sr$ present	0.711425	0.708319	0.707057	0.711931	0.708523	0.710432
error 2 s	0.000022	0.000021	0.000017	0.000044	0.000044	0.000032
$^{87}Sr/^{86}Sr$ initial*	0.711169	0.708178	0.706842	0.711691	0.708347	0.701389
εSr** at T	91.6	49.2	30.2	99.1	51.5	76.9
Nd ppm	47.09	64.73	24.09	50.88	43.05	59.56
Sm ppm	7.57	9.99	4.04	8.74	7.88	11.24
$^{143}Nd/^{144}Nd$ present	0.511722	0.511605	0.512053	0.511726	0.512031	0.512028
$^{147}Sm/^{144}Nd$	0.0972	0.0932	0.1013	0.1037	0.11060	0.11411
$^{143}Nd/^{144}Nd$ at T	0.511722	0.511605	0.512053	0.511726	0.512006	0.512028
εNd (t)	-16.9	-19.2	-10.5	-16.8	-11.5	-11.1
T_{DM} Ga	1.86	1.95	1.49	1.97	1.65	1.72

* Initial $^{87}Sr/^{86}Sr$, εSr (t) and εNd (t) are calculated at 38 Ma for Bingham rocks and 33 Ma for Tintic rocks

** Bulk earth values used are $^{87}Sr/^{86}Sr = 0.704755$ and $^{87}Rb/^{86}Sr = 0.0827$ (Allegre et al., 1983)

The younger volcanic suite contains the most differentiated samples, has a different source, and reflects evolutionary processes.

Origin of Compositional Variation

Fractional crystallization. Several fractional crystallization models were evaluated to test mechanisms for deriving differentiated rocks from various primitive parents. To test the effects of possible olivine fractionation, calculations were made modeling the incremental extraction of 5 wt percent olivine using the method of Nixon (1988) and appropriate Fe/Mg and Ni values. The calculations show that Mg and Ni concentrations of the most primitive nepheline minette (Tick 44; 15.2 wt % MgO and 346 ppm Ni) would change to 12 wt percent MgO and 170 ppm Ni (20 and 50% depletion, respectively) after extraction of 5 wt percent olivine. None of our samples contain such concentrations (Figs. 6 and 7) suggesting that olivine fractionation alone was not important in controlling the concentration of MgO and Ni in the Bingham magmas.

Major-element modeling of fractional crystallization was undertaken using mass balance calculations (Stormer and Nicholls, 1978) and a single-stage, least squares fit of phenocryst compositions and whole-rock chemical analyses as reported in Waite (1996). Using the most primitive nepheline minette as a parent, and a shoshonite with higher SiO_2 as a daughter, modeling produced a relatively good fit ($r^2 = 0.71$, where r^2 equals the sum of the squares of the residuals). Phases used in this model were clinopyroxene, magnetite, olivine, and quartz. Using other phase combinations did not improve the fit. Attempts at using the shoshonite as a parent, and an andesite from the older volcanic suite as a daughter, resulted in a very poor fit ($r^2 = 3.5$).

Trace-element modeling was undertaken using Rayleigh fractionation along with phase proportions from the major-element models and modal analyses, combined with mineral/melt partition coefficients from the literature. Trace-element modeling of Cr and Rb behavior (Figs. 12 and 13) demonstrates that the nepheline minette magma is not related to the other rock suites by fractionation of the observed phases in modal proportions. In contrast, the shoshonites lie on mixing trends between the younger volcanic suite and nepheline minette series (Fig. 12). The elemental trends in the younger volcanic suite are curved and thus inconsistent with simple mixing.

To further test the validity of our major-element model, the percentage of the phases obtained from the major-element model was used to determine bulk partition coefficients for trace-element models. Fractionation curves were then plotted (Waite, 1996). From both the major-element and the trace-element models, strong evidence exists that the nepheline minette did not fractionate to form the other suites. Fractionation may have controlled the compositional variations within the suites.

Magma mixing. Linear trends on Harker variation diagrams (Figs. 6 and 7) are consistent with magma mixing in the older volcanic series. The older volcanic suite has higher MgO, CaO, Fe_2O_3, Ni, and generally lower Cu contents (except for where Cu has been enriched through mineralization) than the other suites. Mixing between the nepheline minette and the older volcanic suite, combined with fractional crystallization, may be the cause of the scatter in the trace-element data.

If fractional crystallization was solely responsible for the compositional trends in the older volcanic suite, the

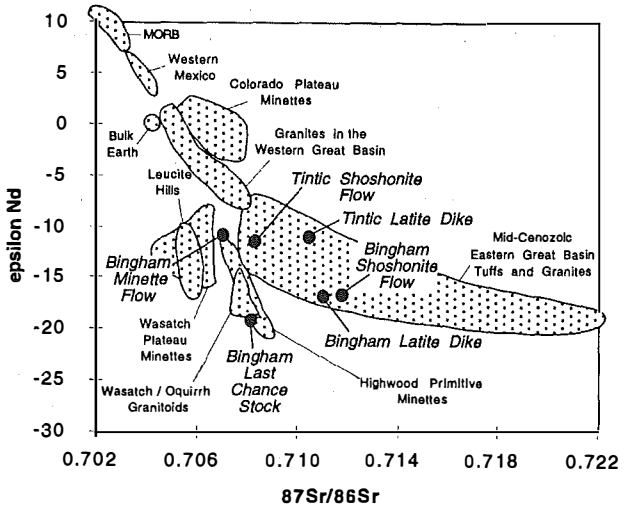

FIG. 11. Sr and Nd isotope plot for Bingham and Tintic samples. Isotope ratios for the nepheline minette flow falls within the field of Wasatch plateau minettes (Tingey et al, 1991) and also along the trend of values for minettes from Highwood, Montana (O'Brien et al., 1991). Sr and Nd isotope ratios for the Last Chance stock are similar to those found by Farmer and DePaolo (1983) for Oquirrh and Wasatch granites. Bingham latite and shoshonite isotope ratios are similar to other mid-Cenozoic intermediate and silicic rocks and granites of the eastern Great Basin (Christiansen, E.H., unpub. data; Farmer and DePaolo, 1983; Grunder and Feeley, 1989).

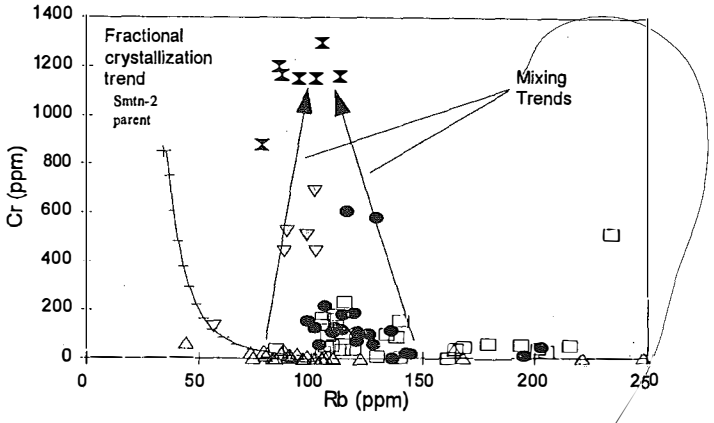

FIG. 12. Cr versus Rb diagram shows fractional crystallizaion and mixing trends for the Bingham samples.

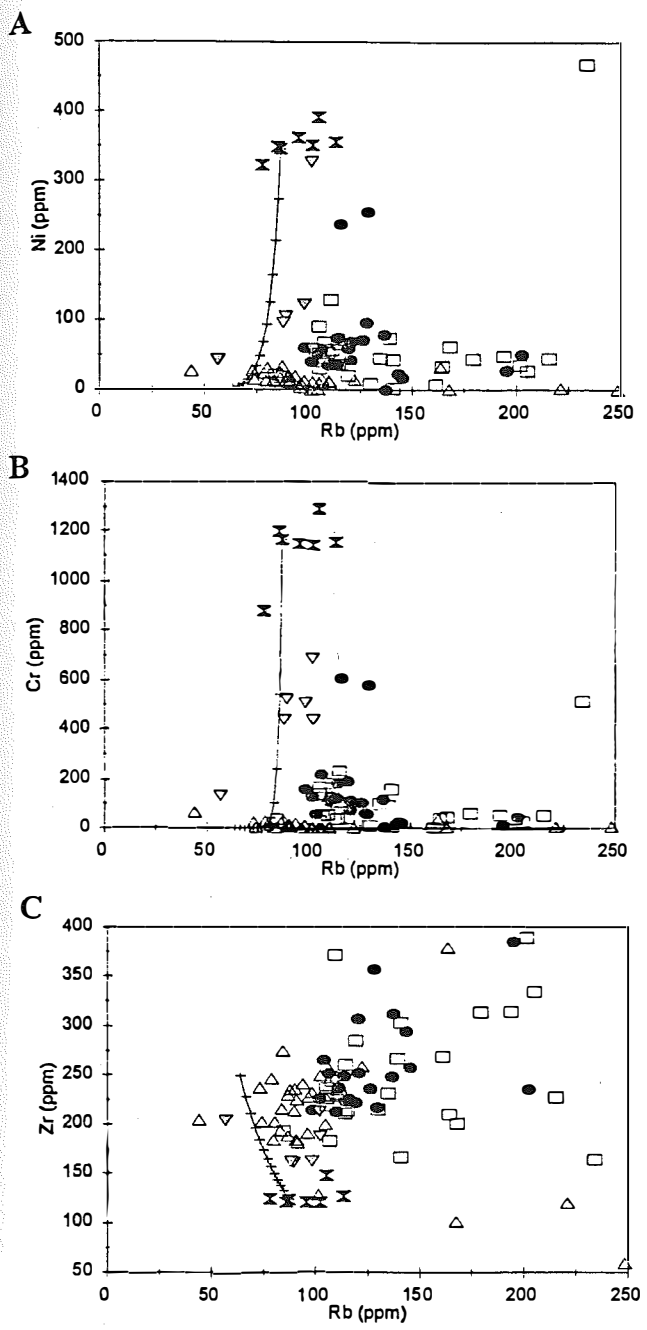

FIG. 13. A-C Graphs showing trace-element modeling trends using results from the major-element modeling versus the composition of the various Bingham suites. The solid line with + marks is the fractionation trend. Each + represents 5% fractionation. (A) Ni versus Rb diagram showing the trend produced by fractionation of clinopyroxene, magnetite, biotite and olivine from a nepheline minette parent. Partition coefficients of $D_{Ni}=1.30$ and $D_{Rb}=5.55$ were calculated for the assemblage that includes clinopyroxene, magnetite, biotite and olivine. The resulting fractionation curve does not go through the shoshonite daughter from the nepheline minette parent. (B) D_{Cr} fractionating phases as used in (A) and (B) also shows that this model does not work.

concentrations of highly compatible elements, such as Cr, would strongly and systematically decrease with increasing SiO_2. However, most samples of the older volcanic and intrusive suites from Bingham have higher Cr concentrations than the younger suite at similar SiO_2 (Fig. 14). High Cr values in these samples suggest that they most likely represent mixed magmas as also shown by petrographic evidence of mixing.

Magma mixing may change sulfur and oxygen fugacities or iron content enough to cause precipitation of magmatic sulfides (Keith et al., 1991). In addition, the solubility of sulfur is greater in mafic melts than in silicic melts. Mixing may therefore have caused formation of Ni-rich magmatic sulfides.

Assimilation-fractional crystallization. As discussed previously, a few samples of the older volcanic suite and the intrusive suite show partially fused and resorbed xenoliths of Oquirrh Group quartzite. Assimilation is also suggested by resorption textures seen in the phenocrysts. However, the major- and trace-element models give strong evidence that the lavas of the older volcanic series were not formed simply by assimilation of Oquirrh Group quartzite.

Magma Genesis

As previously stated, it is unlikely that the nepheline minette magma was the parental magma by fractional crystallization for the dominant volume of the older series of latitic/monzonitic magmas at Bingham. Compositional relationships also preclude the nepheline minette magma from being the parent for the younger volcanic suite. Several lines of evidence suggest diverse sources and perhaps tectonic settings for the latitic/monzonitic magmas in the Bingham mining district.

Müller et al. (1992) distinguished five subgroups of mafic, potassic volcanic rocks generated in distinctive tectonic settings based on geochemical composition. These settings are: within-plates, continental arcs, postcollisional arcs, initial oceanic arcs, and late oceanic arcs. Discrimination diagrams for the mafic Bingham samples show that the nepheline minette samples have arc-related as well as within-plate characteristics (Fig. 15). The within-plate field character of the nepheline minette magma suggests the possibility that the mafic magma may have impinged upon the system during a time of minor extension contemporaneous with subduction-related magmatism. Generation of "within-plate" magmas is typically thought to require upwelling and decompressional melting of asthenosphere in areas of continental lithospheric attenuation (McKenzie and Bickle, 1988), a process that may follow long periods of subduction-related magmatism (Hole et al., 1995). The trace-element and isotopic compositions of the nepheline minette suggest that the magma formed by partial melting of the lower lithosphere or metasomatized mantle. The relatively small volumes of the nepheline minette suggest that such melting may have been localized and of a small degree. Melts

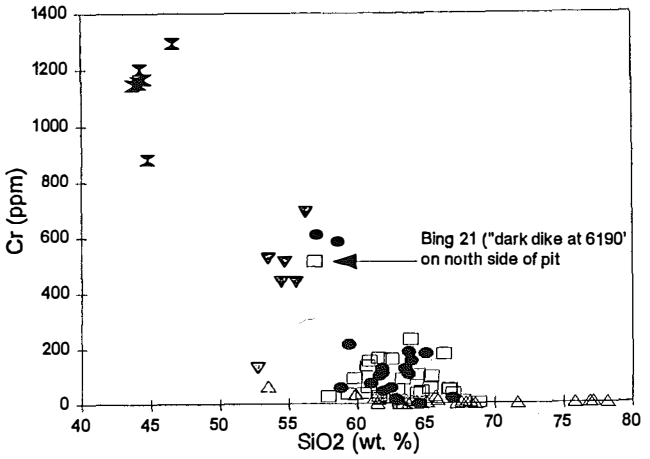

FIG. 14. Cr versus SiO_2 variation diagram showing that the older volcanic unit and intrusive unit have higher Cr values than the younger unit at similar SiO_2. If fractionation had controlled Cr contents in the Bingham magmas, Cr values would be low for all the latite and monzonite units.

so derived would tend to reflect any heterogeneities present in the source region.

Plate reconstructions show that subduction was occurring along the western edge of North America during the Eocene and Oligocene (Severinghaus and Atwater, 1990). However, the prominent east-west alignment of the Stockton-Park City intrusive belt, the similar ages of intrusions along the belt, and the presence of an inferred Archean-Proterozoic suture, all suggest the possibility of mantle melting in a tensional environment (Ballantyne et al., 1995). Details of the actual tectonic setting or stress orientations for the calc-alkaline and the alkaline magmatism near the Bingham porphyry Cu deposit are unknown, but may be related to both active subduction and localized crustal extension related to back-arc spreading. Even a mildly extensional tectonic regime, as proposed for central Utah during the Eocene and Oligocene (Presnell, 1992; 1997), may suffice to allow primitive, alkaline magmas intermittently to erupt or underplate subduction-related calc-alkaline magma chambers.

So where did the mafic, alkaline magmas at Bingham come from? Many recent studies have documented the occurrence of alkaline magmas in convergent margins worldwide, where unusual tectonic regimes have led to rifting and extension of the arc crust (e.g. Box and Flower, 1989). Richards et al. (1990) suggested that alkalic magmatism at Porgera, New Guinea, may have formed in response to changes in tectonic setting and subduction behavior shortly before or during the onset of an early Pliocene collision event. When a subcontinental lithospheric mantle that has been previously metasomatized undergoes extension and/or heating the earliest mafic melts generated may be rich in volatiles and potassium (Gibson et al., 1995). Volatile-rich, small-fraction melts tap some of the most extreme products of mantle enrichment processes and usually have high concentrations of incompatible trace elements, such as occur in the Bingham mafic lava samples. If extension did occur, the primitive nepheline minette magma may have risen separately from its source to intersect high-level magma systems, or it may have erupted elsewhere in the region. If extension did not occur, the nepheline minette magma fraction would have been assimilated into subduction-related magma passing through the lithospheric mantle.

The mafic alkaline magma from the Bingham mining district may have originated from partial melting of the metasomatized lithospheric mantle wedge above the subducting Farallon plate. Bailey et al. (1989) proposed that metasomatism of the mantle wedge by slab melts or fluids of a felsic and alkaline composition is necessary to account for normative nepheline, K- and LILE- enriched basalts, including shoshonites. Magmas produced by melting of such metasomatized regions are relatively oxidized, as shown by high Mg/Fe ratios in rocks and minerals and by early crystallization of abundant magnetite (Carmichael, 1991). They are also often depleted in heavy rare earth elements, which is explained by the retention of garnet in the mantle or strong LREE enrichment accompanying metasomatism. All of the nepheline minette samples contain normative nepheline, magnetite, and strongly Mg-rich mafic phenocrysts, which suggests that these magmas were relatively oxidized. Their low SiO_2, coupled with high K and Na, is consistent with generation of unusually low degrees (<1%) of partial melting as suggested by experimental evidence for the generation of normative nepheline alkaline magmas (Green, 1970).

Luhr et al. (1989) developed a model for generation of lamprophyres in the subduction-related western Mexican Volcanic Belt that could apply to any arc environment. Low-volume melts, concentrating metasomatic vein components in the sub-arc mantle, are probably generated in most subduction-related arcs. Typically these volatile-rich melts freeze during ascent to form classic lamprophyric dikes in the arc crust. These melts are able to erupt at the surface only in arcs, such as the western Mexican Volcanic Belt, where extensional tectonic stresses are superimposed on the convergent regime (Luhr et al., 1985). This may have occurred in the Bingham mining district. As noted by Seedorff (1991), extension in porphyry-related deposits provides opportunity for the development of dikes and veins; it also controls the compositions of magmas and the incursion of meteoric water. Extension also may have occurred in an intra-arc setting during waning plate convergence or through intraplate gravitational spreading driven by thermal relaxation and upwelling of mantle basalt.

If the alkalic volcanism at Bingham is related to intra-arc rifting, there should be a cycle of volcanism from pre-rift tholeiitic or calc-alkaline volcanism, interrupted by an alkalic phase during the onset of intra-arc spreading. This would be followed by a progressive return to tholei-

itic or calc-alkaline compositions after rifting (Bloomer et al., 1989). This cycle may be represented in the Bingham mining district by emplacement of the calc-alkaline Last Chance Stock and older volcanic suite, interrupted by the alkaline, nepheline minettes and shoshonite flows, and then calc-alkaline volcanism of the younger suite.

Moore (1993) modeled the petrogenesis of the East Tintic volcanic field (35–32 Ma) that is 45 km south of the Bingham mining district. His model also required the presence of two distinct magma suites. The older suite was low-silica rhyolite and andesite(?) that formed, at least in part, by anatexsis of the lower crust. These batches of magma were succeeded by, and mixed with, a shoshonite-trachyte series of magma. Intrusions that formed by mixing of these magma suites in shallow-level magma chambers are related to formation of ore deposits; intrusions that formed before arrival of the shoshonite-trachyte suite are barren.

Ore Genesis

Mafic alkaline magmas are often rich in sulfur (2,000–4,000 ppm; Carmichael and Ghiorso, 1986), but quantifying how much sulfur was in the pre-erupted magma is problematic, because sulfur degassing after eruption removes a large portion of the total sulfur budget of the lavas. Keith et al. (1993) proposed that the most primitive, shoshonitic magma in the East Tintic volcanic field was not sulfide-saturated when it arrived at shallow crustal levels. This would prevent depletion of S and chalcophile metals. As the S-rich mafic magma mixed with more differentiated magma, or SO_2 fluxing occurred, magmatic sulfide blebs were created and ore-related chalcophile metals were temporarily sequestered. Such mixing may be accompanied by a net decrease in oxygen fugacity for the mafic constituent, which might then lower the solubility of S in the melt and increase the proportion of immiscible sulfide (Carroll and Rutherford, 1985; Keith et al., 1991).

Mass balance calculations using the compositions of the sulfide inclusions and host rocks from Bingham indicate that the Bingham magmatic sulfide inclusions contain essentially all of the S, As, Cu, and Ag in the rocks (Keith et al., 1995). Gold is likely sequestered to a similar, but undetectable, extent (Hattori, 1987). Some loss of Cu, Ag, and Au from the magma may have occurred after eruption, but it is probably minor in these glassy rocks. Cu, Ag, and Au would be expected to partition strongly into a sulfide phase as they are chalcophile elements.

One of the most significant characteristics of magmatic sulfides is the fact that they are not commonly preserved in slowly cooled lavas and intrusions. The timing, extent, and mechanisms for their removal from magmas are not well known, but it is unlikely that significant amounts of Cu-Ag-Au-bearing ore fluids can be produced from sulfide-saturated magmas without at least partial removal of the magmatic globules. Candela and Holland (1986) and Candela (1989b) consider the possibility that

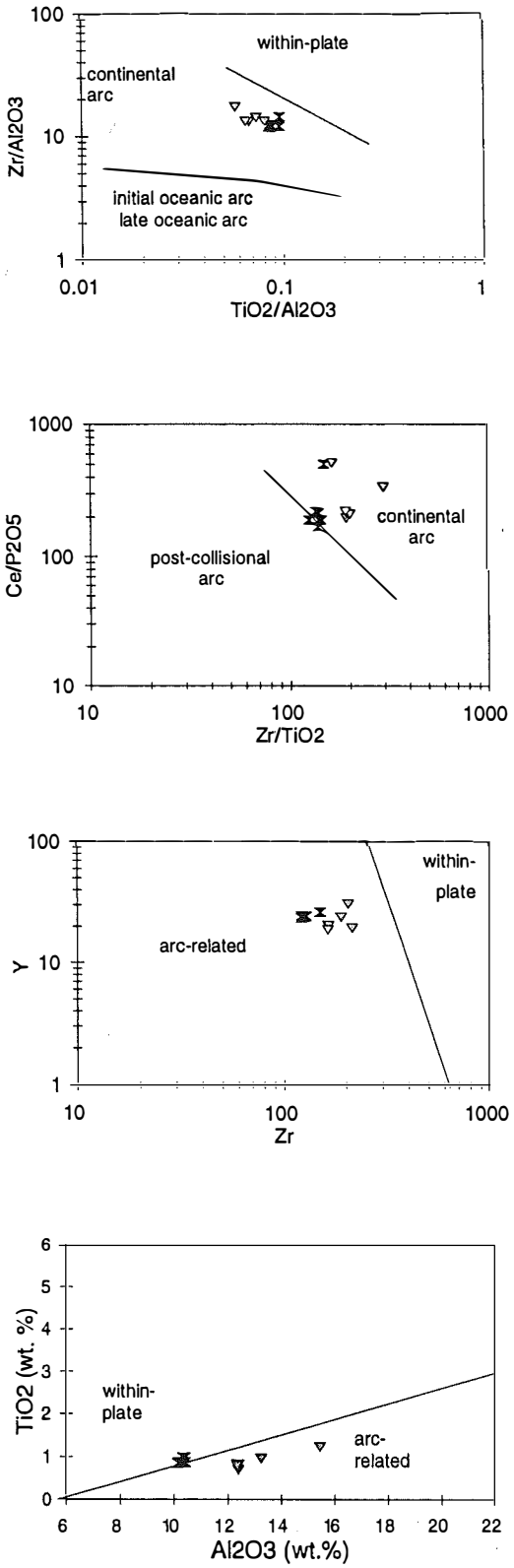

FIG. 15. Tectonic discrimination diagrams comparing Zr/Al_2O_3 versus TiO_2/Al_2O_3; Ce/P_2O_5 versus Zr/TiO_2; TiO_2 versus Al_2O_3; and Y versus Zr. These plots show those samples that have "continental," "within-plate," and "arc-related" characteristics.

magmatic pyrrhotite may sequester Cu and then become destabilized after vapor saturation. Candela and Holland (1986) propose that loss of a SO_2-rich vapor from the magma would cause oxidation of pyrrhotite globules according to the following reaction:

$$FeS_{po} + 3/2O_2 = FeO_l + SO_{2v}$$

All oxidized globules that we have analyzed contain Fe_2O_3 rather than FeO, but the idea of magmatic oxidation of sulfides seems feasible. Many lines of evidence indicate that a S-rich pre-eruptive fluid phase may be present in sub-volcanic chambers (Luhr et al., 1984; Westrich and Gerlach, 1992; Lowenstern, 1993). Periodic loss of a S-rich fluid may lower the S and H_2O content of the melt and destabilize the sulfides. Upward volatile fluxing of a SO_2-rich fluid may also oxidize the sulfides (Hattori, 1993). Alternatively, the substantial pressure decrease and loss of sulfurous gases and H_2O that may accompany the emplacement of subvolcanic intrusions may also lead to resorption of sulfides. Lowenstern (1993) demonstrates that crystallization-induced volatile saturation, or "second-boiling" may not be a prerequisite for the creation of metal-bearing hydrothermal fluids. Instead, volatile saturation may occur due to the depressurization combined with the presence of low solubility gases such as CO_2 and SO_2. Clearly, magmatic sulfides that consist of more than 50 mole percent of a common volcanic gas may be "ephemeral" in a magma chamber.

For Bingham, we suggest that first, a wet latitic magma formed from mixtures of crustal and subduction-related, mantle-derived magma and was emplaced in a high-level magma chamber (Fig. 16); then, mild extensional tectonism allowed quick passage through the crust for small batches of primitive nepheline minette magma. This nepheline minette magma was S- and Cu-rich and may have originated from partial melting of a metasomatized lithospheric mantle. Huppert et al. (1982) suggest mixing can occur when a wet, under-saturated mafic magma impinges upon the base of a magma chamber containing more differentiated magma. Turbulent transfer of heat between the mafic magma and the overlying silicic magma could have led to crystallization and exsolution of volatiles in the lower layer. Alternately, the mafic magma might have been volatile-saturated at low pressure, in which case the bulk density of the vesiculating mafic magma could have become equal to that of the overlying magma causing mixing to occur. This mechanism is most probable in the low-pressure environment of a high-level magma chamber. The arrival of mafic, alkaline, volatile-rich and oxidized magma (represented by the nepheline minette) at the base of a calc-alkaline magma chamber may have been a critical factor in the formation of the Bingham Cu-Au-Mo deposit (Keith et al., 1995).

Conclusions

This paper documents important new findings concerning the volcanic and intrusive rocks associated with the Bingham Cu porphyry deposit of central Utah. Besides the dominant calc-alkaline magma in the Bingham mining district, small volumes of primitive, alkaline magma also erupted (Mg # >65). A model is presented that demonstrates how these primitive magmas may have played an important role in the development of this large porphyry copper deposit. These nepheline minettes contain high concentrations of volatiles, LILE, and LREE, but relatively low concentrations of Ti, Nb, and Zr on mantle-normalized diagrams. The silica-undersaturated nature, high abundances of volatiles, compatible and incompatible elements, and negative Nb and Ti anomalies in the nepheline minettes suggest that they might be primary melts produced by low degrees of melting of a metasomatized, lithospheric mantle source. Olivine from the nepheline minettes is highly magnesian with Fo_{85-92}. These olivine compositions fall in the range (Fo_{88-94}) expected for primitive magmas derived from "normal" mantle and are near the compositions of olivine (Fo_{87-94}) in phlogopite-bearing mantle inclusions.

The younger volcanic suite most likely vented from a separate, younger magmatic system, distinct from that associated with the Bingham intrusions and older volcanic suites. Differences between the older suite and the younger suite include stratigraphic position and chemical composition. However, the older and younger volcanic suites contain similar mineral assemblages.

Fractional crystallization, magma mixing, and assimilation played important roles in determining the composition of the Bingham mining district magmas in this open, ore-related system. The nepheline minette flows are not related to the other volcanic and intrusive suites by fractional crystallization, but mixing of the minette with magma similar in composition to the younger volcanic suite could have created the magma of the older suite. The nepheline minette magmas are those most closely related to the Cu-Au-Mo mineralization. Trace-element models indicate that late mineralized dikes may have been formed by mixing of about 10 percent minette magma and 90 percent calc-alkaline magma.

The sulfide-undersaturated character of the primitive alkaline magmas allowed them to rise through the crust with almost no loss of S, Cu, or other chalcophile metals. Sulfide saturation of the latitic magma most likely occurred when the mafic magmas mixed with cooler more silicic magma. This indicates that most of the Cu and chalcophile metals were initially sequestered within magmatic sulfide blebs. Crystallization alone may not be sufficient to form metal-rich magmatic ore fluids capable of forming deposits such as the Bingham porphyry deposit. Pressure decrease, possibly associated with eruption, intrusion, or loss of magmatic volatiles would initiate resorption and oxidation of sulfide blebs and release the sequestered metals and sulfur to the hydrothermal system. Petrography of comagmatic dikes and intrusions indicates that resorption and oxidation of the sulfides may have made their metal content available to the

hydrothermal system. Degassing of underplated and mixed minette magma may have contributed large amounts of sulfur, volatiles and metals to the ore-forming system.

Acknowledgments

Partial financial support for this project came from NSF grant EAR-9114980. We thank Kennecott Utah Copper Corporation for permission to collect samples; Jaren Swensen, Jed Maughan, and Geoff Ballantyne for guiding our sampling in the Bingham mine; and Geoff Ballantyne, David John, and Paula Wilson for reviews. We thank Camp Williams for permission to work on their property and Captain Dutton for guiding us on several trips. Appreciation is extended to Jean Baker for help in collecting the samples. We thank T.C. McCarthy for electron microprobe analyses of the silicates. We are grateful to Daniel Maughan and Mike Dorais for electron microprobe data.

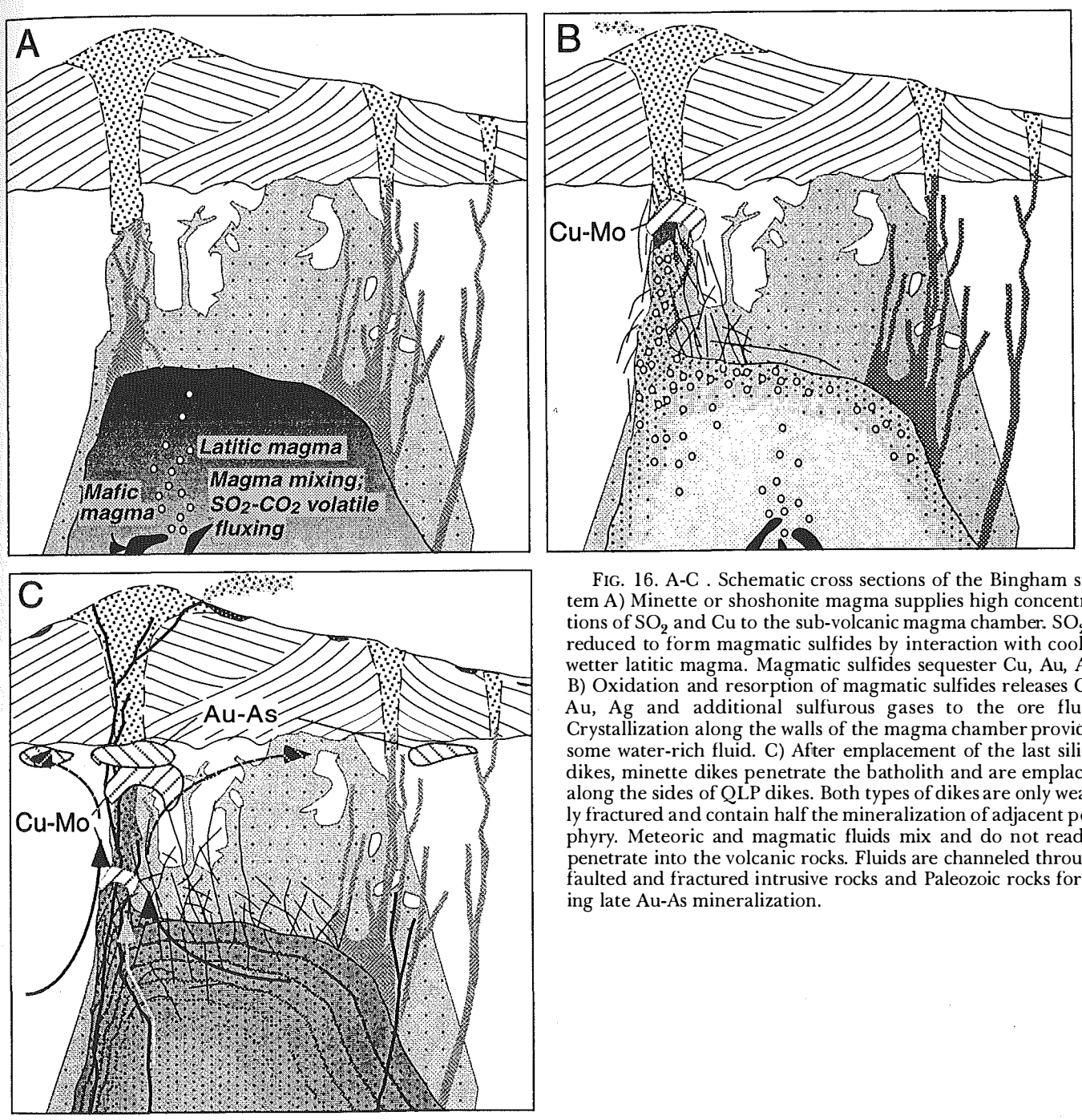

FIG. 16. A-C . Schematic cross sections of the Bingham system A) Minette or shoshonite magma supplies high concentrations of SO_2 and Cu to the sub-volcanic magma chamber. SO_2 is reduced to form magmatic sulfides by interaction with cooler, wetter latitic magma. Magmatic sulfides sequester Cu, Au, Ag. B) Oxidation and resorption of magmatic sulfides releases Cu, Au, Ag and additional sulfurous gases to the ore fluid, Crystallization along the walls of the magma chamber provides some water-rich fluid. C) After emplacement of the last silicic dikes, minette dikes penetrate the batholith and are emplaced along the sides of QLP dikes. Both types of dikes are only weakly fractured and contain half the mineralization of adjacent porphyry. Meteoric and magmatic fluids mix and do not readily penetrate into the volcanic rocks. Fluids are channeled through faulted and fractured intrusive rocks and Paleozoic rocks forming late Au-As mineralization.

References

Allegre, C.J., Hart, S.R., and Minster, J.F., 1983, Chemical structure and evolution of the mantle and continents determined by inversion of Nd and Sr isotopic data, II, Numerical experiments and discussion: Earth and Planetary Science Letters, v. 66, p. 191–213.

Babcock, R.C., Jr., Ballantyne, G.H., and Phillips, C.H., 1995, Summary of the geology of the Bingham district, Utah, *in* Pierce, F.W., and Bolm, J.G., eds., Porphyry copper deposits of the American Cordillera: Tuscon, Arizona Geological Society Digest 20, p. 316–335.

Bailey, J.C., Frolova, T.I., and Burikova, L.A., 1989, Mineralogy, geochemistry, and petrogenesis of Kurile island-arc basalts: Contributions to Mineralogy and Petrology, v. 102, p. 265–280.

Ballantyne, G.H., Maughan, C.J., and Smith, T., 1995, The Bingham copper-gold-molybdenum deposit, Utah: Why Bingham is a "Super-Giant", *in* Controls on the scale of hydrothermal activity associated with orogenic magmatism: QminEx Symposium, Queen's University, April 25–27, p. 300–315.

Barr, D.L., 1993, Time, space and composition patterns of middle Cenozoic mafic to intermediate composition lava flows of the Great Basin, western U.S.A.: Unpublished M.S. thesis, Provo, Utah, Brigham Young University, 68 p.

Basaltic Volcanism Study Project, 1981, *in* Basaltic volcanism on the terrestrial planets, New York, Pergamon, 1286 p.

Best, M.G., and Christiansen, E.H., 1991, Limited extension during peak Tertiary volcanism, Great Basin of Nevada and Utah: Journal of Geophysical Research v. 96, p. 13509–13528.

Best, M.G., Christiansen, E.H., Deino, A.L., Grommé, C.S., McKee, E.H., and Noble, D.C., 1989, Excursion 3A: Eocene through Miocene volcanism in the Great Basin of the western United States, *in* Chapin, C.E., and Zidek, J., eds., Field excursions to volcanic terranes in the western United States, Vol II: Cascades and Intermountain West: New Mexico Bureau of Mines and Mineral Resources Memoir 47, p. 91–133.

Bloomer, S.H., Stern, R.J., Fisk, E., and Geschwind, C.H., 1989, Shoshonitic volcanism in the Northern Mariana Arc 1. Mineralogic and major and trace element characteristics: Journal of Geophysical Research, v. 94, p. 4469–4496.

Box, S.E., and Flower, M.F.J., 1989, Introduction to special section on alkaline arc magmatism: Journal of Geophysical Research, v. 94, p. 4467–4468.

Bray, R.E., 1969, Igneous rocks and hydrothermal alteration at Bingham, Utah: Economic Geology, v. 64, p. 34–49.

Burnham, C.W., 1979, Magmas and hydrothermal fluids *in* Barnes, H.L., ed., Geochemistry of hydrothermal ore deposits, New York, John Wiley, p. 71–136.

Candela, P.A., 1989a, Felsic magmas, volatiles, and metallogenesis, *in* Whitney, J.A., and Naldrett, A.J., eds., Ore deposition associated with magmas, Reviews in Economic Geology, v. 4, p. 223–233.

—— 1989b, Magmatic ore-forming fluids: thermodynamic and mass transfer calculations of metal concentrations, *in* Whitney, J.A., and Naldrett, A.J., eds., Ore deposition associated with magmas, Reviews in Economic Geology, v. 4, p. 203–221.

Candela, P.A., and Holland, H.D., 1986, A mass transfer for copper and molybdenum in magmatic hydrothermal systems: The origin of porphyry-type ore deposits: Geochimica et Cosmoschimica Acta, v. 81, p. 1–19.

Carmichael, I.S.E., 1991, The redox states of basic and silicic magmas: a reflection of their source regions?: Contributions to Mineralogy and Petrology, v. 106, p. 129–141.

Carmichael, I.S.E., and Ghiorso, M.S., 1986, Oxidation-reduction relations in basic magma: a case for homogenous equilibria: Earth and Planetary Science Letters, v. 78, p. 200–210.

Carroll, M.R., and Rutherford, M.J., 1985, Sulfide and sulfate saturation in hydrous silicate melts: Journal of Geophysical research, v. 90, supplement C601–C612.

Cline, J.S., and Bodnar, R.J., 1991, Can economic porphyry copper mineralization be generated by a typical calc-alkaline melt?: Journal of Geophysical Research, v. 96, p. 8113–8126.

Craig, J.R., and Kullerud, G., 1969, Phase relations in the Cu-Fe-Ni-S system and their application to magmatic ore deposits: Economic Geology Monograph 4, p. 344–358.

Craig, J.R., and Scott, S.D., 1974, Sulfide phase equilibria *in* Ribbe, P.H., ed., Sulfide mineralogy: Mineralogical Society of America Short Course Notes, Blacksburg, Virginia, Southern Printing Company, p. CS1–104.

Cross, T.A., and Pilger, R.H., 1978, Constraints on absolute motion and plate interaction inferred from Cenozoic igneous activity in the western United States: American Journal of Science, v. 278, p. 865–902.

DePaolo, D.J., 1981, Nd in the Colorado Front Range and implications of crust formation and mantle evolution in the Proterozoic: Nature, v. 291, p. 193–196.

Erickson, A.J., Jr., 1976, The Uinta-Gold Hill trend: an economically important lineament, *in* Hogdson, R.R., ed., Proceedings of the First International Conference on the New Basement Tectonics: Utah Geological Association, p. 126–138.

Erlank, A.J., Waters, F.G., Hawkesworth, C.J., Haggerty, S.E., Allsop, H.L., Rickard, R.S., and Menzies, M.A., 1987, Evidence for mantle metasomatism in peridotite nodules from the Kimberley Pipes, South Africa *in* Menzies, M.A., and Hawkesworth, C.J., eds., Mantle metasomatism: San Diego, California, Academic, p. 221–331.

Farmer, G.L., and DePaolo, D.J., 1983, Origin of Mesozoic and Tertiary Granites in the western United States and implications for pre-Mesozoic crustal structure: 1. Nd and Sr isotopic studies in the geocline of the northern Great Basin: Journal of Geophysical Research, v. 88, p. 3379–3401.

Gans, P.B., Mahood, G.A., and Schermer, E., 1989, Synextensional magmatism in the Basin and Range province: A case study from the eastern Great Basin: Geological Society of America Special Paper 233, p. 1–53.

Gibson, S.A., Thompson, R.N., Leonardos, O.H., Dickin, A.P., and Mitchell, J.G., 1995, The late Cretaceous impact of the Trindade mantle plume: evidence from large-volume, mafic, potassic magmatism in SE Brazil: Journal of Petrology, v. 36, p. 189–229.

Gilluly, J., 1932, Geology and ore deposits of the Stockton and Fairfield quadrangles, Utah: U.S. Geological Survey Professional Paper 173, 171 p.

Green, D.H., 1970, A review of experimental evidence on the origin of basaltic and nephelinitic magmas: Physics of the Earth and Planetary Interiors, v. 3, p. 221–235.

—— 1971, Compositions of basaltic magmas as indicators of conditions of origin: Applications to oceanic volcanism: Philosophical Transactions of the Royal Society of London, v. 268, p. 707–725.

Grunder, A.L., and Feeley, T.C., 1989, Evidence for crustal and mantle sources of Tertiary, extension-related volcanism in east-central Nevada [abs.]: Continental magmatism abstracts:

New Mexico Bureau of Mines and Mineral Resources Bulletin, 116 p.

Hattori, K., 1987, Magnetic felsic intrusions associated with Canadian Archean gold deposits: Geology, v. 15, p. 1107–1111.

_____1993, High-sulfur magma, a product of fluid discharge from underlying mafic magma: Evidence from Mount Pinatubo, Philippines: Geology, v. 21, p. 1083–1086.

Helm, J.M., 1994, Structure and tectonic geomorphology of the Stansbury Fault zone, Tooele County, Utah, and the effect of crustal structure on Cenozoic faulting patterns: Unpublished M.S. thesis, Salt Lake City, Utah, University of Utah, 128 p.

Hole, M.J., Saunders, A.D., Rogers, G., and Sykes, M.A., 1995, The relationship between alkaline magmatism, lithospheric extension and slab window formation along continental destructive plate margins, *in* Smellie, J.L., ed., Volcanism associated with extension at consuming plate margins: Geological Society Special Publication no. 81, p. 169–191.

Hook, C.J., 1995, Magmatic sulfides in intermediate to mafic volcanic rocks contemporaneous with ore-related plutonism at Bingham, Utah: Unpublished M.S. thesis, Athens, Georgia, University of Georgia, 178 p.

Huppert, H.E., Sparks, R.S.J., and Turner, J.S., 1982, Effects of volatiles on mixing in calc-alkaline magma systems: Nature, v. 297, p. 554–557.

James, A.H., Smith, W.H., and Welsh, J.E., 1961, General geology and structure of the Bingham mining district, Utah: Utah Geological Society Guidebook 16, p. 101–119.

John, E.C., 1978, Mineral zones in the Utah Copper orebody: Economic Geology, v. 73, p. 1250–1259.

Keith, J.D., Dallmeyer, R.D., Kim, C.S., and Kowallis, B.J., 1991, The volcanic history and magmatic sulfide mineralogy of latites of the central east Tintic Mountains, Utah, *in* Raines, G.L., Lisle, R.E., Schafer, R.W., and Wilkinson, W.H., eds., Geology and ore deposits of the Great Basin, Geological Society of Nevada, p. 461–483.

Keith, J.D., Moore, D.K., Tingey, D.G., Barr, D.L., Christiansen, E.H., Whitney, J.A., and Cannan, T.M., 1993, The role of mafic alkaline magmas and magmatic sulfides in ore genesis: examples from the Bingham mining district and the East Tintic Mountains, Utah [abs.]: Geological Society of America Abstracts with Programs, v. 25, p. 61.

Keith, J.D., Whitney, J.A., Cannan, T.M., Hook, C.J., and Hattori, K., 1995, The role of magmatic sulphides and mafic alkaline magmatism in the formation of giant porphyry and vein systems: examples from the Bingham and Tintic mining districts, Utah, *in* Controls on the scale of hydrothermal activity associated with orogenic magmatism: QminEx Symposium, Queen's University, April 25–27, p. 316–339.

Lanier, G., John, E.C., Swensen, A.J., Reid, J., Bard, C.E., Caddey, S.W., and Wilson, J.C., 1978, General geology of the Bingham Mine, Bingham Canyon, Utah: Economic Geology, v. 73, p. 1223–1241.

Le Maitre, R.W., 1989, A classification of igneous rocks and glossary of terms, Oxford, Blackwell.

Link, P.K., Christie-Blick, N., Devlin, W.J., Elston, D.P., Horodyski, R.J., Levy, M., Miller, J.M.G., Pearson, R.C., Prave, A., Stewart, J.H., Winston, D., Wright, L.A., and Wrucke, C.T., 1993, Middle and late Proterozoic stratified rocks of the western U.S. Cordillera, Colorado Plateau, and Basin and Range province *in* Reed, J.C., Jr., Bickford, M.E., Houston, R.S., Link, P.K., Rankin, D.W., Sims, P.K., and Van Schmus, W.R., eds., Precambrian: Conterminous U.S.: Geological Society of America, The Geology of North America, v. C-2, p. 463–596.

Lipman, P.W., 1980, Cenozoic volcanism in the western United States: Implications for continental tectonics, *in* Studies in geophysics: Continental tectonics, Washington, D. C., National Academy of Sciences, p. 161–174.

Lofgren, G.E., 1980, Experimental studies on the dynamic crystallization of silicate melts, *in* Hargraves, R.B., ed., Physics of magmatic processes, p. 487–546.

Lowenstern, J.B., 1993, Evidence for a copper-bearing fluid in magma erupted at the Valley of Ten Thousand Smokes, Alaska: Contributions to Mineralogy and Petrology, v. 114, p. 409–421.

Luhr, J.F., Carmichael, I.S.E., and Varecamp, J.C., 1984, The 1982 eruptions of El Chichon volcano, Chiapas, Mexico: mineralogy and petrology of the anhydrite-bearing pumices: Journal of Volcanology and Geothermal Research, v. 23, p. 69–108.

Luhr, J.F., Nelson, S.A., Allen, J.F., and Carmichael, I.S.E., 1985, Active rifting in southwestern Mexico: Manifestations of an incipient eastward spreading-ridge jump: Geology, v. 13, p. 54–57.

Luhr, J.F., Allen, J.F., Carmichael, I.S.E., Nelson, S.A., and Hasenaka, T., 1989, Primitive calc-alkaline and alkaline rock types from the Western Mexican Volcanic Belt: Journal of Geophysical Research, v. 94, p. 4515–4530.

McKee, E.H., Best, M.G., Barr, D.L., and Tingey, D.G., 1993, Potassium-argon ages of mafic and intermediate-composition lava flows in the Great Basin of Nevada and Utah: Isochron/West, v. 60, p. 15–18.

McKenzie, D.P., and Bickle, M.J., 1988, The volume and composition of melt generated by extension of the lithosphere: Journal of Petrology, v. 29, p. 625–679.

Mitchell, R.H., and Platt, R.G., 1984, The Freemans Cove volcanic suite: field relations, petrochemistry, and tectonic setting of nephelinite-basanite volcanism associated with rifting in the Canadian Arctic Archipelago: Canadian Journal of Earth Science, v. 21, p. 428–436.

Moore, D.K., 1993, Oligocene East Tintic volcanic field, Utah: Unpublished M.S. Thesis, Provo, Utah, Brigham Young University, 64 p.

Moore, W.J., 1973a, A summary of radiometric ages of igneous rocks in the Oquirrh Mountains, north-central Utah: Economic Geology, v. 68, p. 97–101.

—— 1973b, Igneous rocks in the Bingham Mining District, Utah: Geological Survey Professional Paper 629-B.

Moore, W.J., and McKee, E.H., 1983, Phanerozoic magmatism and mineralization in the Tooele 1° x 2° quadrangle, Utah: Geological Society of America, Memoir 157, p.183–190.

Moore, W.J., Lanphere, M.A., and Obradovich, J.D., 1968, Chronology of intrusion, volcanism, and ore deposition at Bingham, Utah: Economic Geology, v. 63, p. 612–621.

Müller, D., Rock, N.M.S., and Groves, D.I., 1992, Geochemical discriminations between shoshonitic and potassic volcanic rocks from different tectonic settings: a pilot study: Mineralogy and Petrology, v. 46, p. 259–289.

Nixon, G.T., 1988, Petrology of the younger andesites and dacites of Iztaccihuatl Volcano, Mexico: I. Disequilibrium phenocryst assemblages as indicators of magma chamber processes: Journal of Petrology, v. 29, p. 213–264.

O'Brien, H.E., Irving, A.J., and McCallum, I.S., 1991, Eocene potassic magmatism in the Highwood Mountains, Montana: petrology, geochemistry, and tectonic implication: Journal of Geophysical Research, v. 96, p. 13237–13260.

Ormerod, D.S., Hawkesworth, C.J., Rogers, N.W., Leeman, W.P., and Menzies, M.A., 1988, Tectonic and magmatic transitions in the western Great Basin, USA: Nature, v. 333, p. 349–353.

Perfit, M.R., 1985, Alkalic volcanic rocks from SW Pacific island arcs: subduction or rift related? [abs.]: Geological Society of America Abstracts, v. 17, p. 187.

Presnell, R.D., 1992, Local and regional geology of the Oquirrh Mountains, *in* Wilson, J.R., ed., Field guide to geologic excursions in Utah and adjacent areas of Nevada, Idaho, and Wyoming: Utah Geological Survey Miscellaneous Publication 92-3, p. 293–306.

—— 1997, Structural controls on the plutonism and metallogeny in the Wasatch and Oquirrh Mountains, Utah: Society of Economic Geologists Guidebook No. 29, p. 1–9.

Richards, J.P., Chappell, B.W., and McCulloch, M.T., 1990, Intraplate-type magmatism in a continent-island arc collision zone: Porgera intrusive complex Papua, New Guinea: Geology, v. 18, p. 958–961.

Sato, H., 1977, Nickel content of basaltic magmas: Identification of primary magmas and a measure of the degree of olivine fractionation: Lithos, v. 10, p. 113–120.

Seedorff, C.E., 1991, Magmatism, extension, and ore deposits of Eocene to Holocene age in the Great Basin-Mutual effects and preliminary proposed genetic relationships, in Raines, G.L., Lisle, R.E., Schafer, R.W., and Wilkinson, W.H., eds., Geology and ore deposits of the Great Basin, Geological Society of Nevada, p. 133–178.

Severinghaus, J., and Atwater, T., 1990, Cenozoic geometry and thermal state of subducting slabs beneath western North America, *in* Wernicke, B.P., ed., Basin and Range extensional tectonics near the latitude of Las Vegas, Nevada: Geological Society of America Memoir 176, p. 1–22.

Smith, W.H., 1961, The volcanics of the eastern slopes of the Bingham mining district *in* Cook, D.R., ed., Geology of the Bingham mining district and northern Oquirrh Mountains: Utah Geological Society Guidebook 16, p. 101–119.

Stewart, J.H., and Carlson, J.E., 1976, Cenozoic rocks of Nevada, Map 53, Nevada Bureau of Mines and Geology, Reno.

Stewart, J.H., Moore, W.J., and Zietz, I., 1977, East-west patterns of Cenozoic igneous rocks, aeromagnetic anomalies, and mineral deposits, Nevada and Utah: Geological Society of America Bulletin, v. 88, p. 67–77.

Stone, W.E., Fleet, M.E., and MacRaem, N.D., 1989, Two-phase nickeliferous monosulfide solid solution (mss) in megacrysts from Mount Shasta, California: A natural laboratory for nickel-copper sulfides: American Mineralogist, v. 74, p. 981–993.

Stormer, J.C., and Nicholls, J., 1978, XLFRAC: A program for the interactive testing of magmatic differentiation models: Computers and Geosciences v. 4, p. 143–159.

Thompson, R.N., Morrison, M.A., Hendry, G.L., and Parry, S.J., 1984, An assessment of the relative roles of crust and mantle in magma genesis: An elemental approach: Philosophical Transactions of the Royal Society of London, v. A310, p. 549–590.

Tingey, D.G., Christiansen, E.H., Best, M.G., Ruiz, J., and Lux, D.R., 1991, Tertiary minette and melanephelinite dikes, Wasatch Plateau, Utah: Records of mantle heterogeneities and changing tectonics: Journal of Geophysical Research, v. 96, p. 13529–13544.

Tooker, E.W., and Roberts, R.J., 1961, Stratigraphy of the north end of the Oquirrh Mountains, Utah, *in* Cook, D.R., ed., Geology of the Bingham mining district and northern Oquirrh Mountains: Utah Geological Society Guidebook to the Geology of Utah, no. 16, p. 17–35.

Waite, K.A., 1996, Petrogenesis of the volcanic and intrusive rocks associated with the Bingham porphyry Cu-Mo deposit, Utah: Unpublished M.S. thesis, Provo, Utah, Brigham Young University, 54 p.

Wallace, P., and Carmichael, I.S.E., 1989, Minette lavas and associated leucites from the western front of the Mexican Volcanic Belt: petrology, chemistry and origin: Contributions to Mineralogy and Petrology, v. 103, p. 470–492.

Warnaars, F.W., Smith, W.H., Bray, R.E., Lanier, G., and Shafiqullah, M., 1978, Geochronology of igneous intrusions and porphyry copper mineralization at Bingham, Utah: Economic Geology, v. 73, p. 1242–1249.

Westrich, H.R., and Gerlach, T.M., 1992, Magmatic gas source for the stratospheric SO_2 cloud from the June 15, 1991, eruption of Mount Pinatubo: Geology, v. 20, p. 867–870.

Willden, C.R., 1952, The nature of the igneous-sediment contact in the U. S. mine, Bingham, Utah: Unpublished M.S. thesis, Salt Lake City, University of Utah, 41 p.